

It also must have a rather reactive nucleophile at its active center (probably a cysteine<sup>1c</sup>). These two factors in combination explain why efforts to employ such conjugated analogues have only succeeded at inactivating PDC, but failed to inactivate pyruvate oxidase, pyruvate dehydrogenase, pyruvate-ferredoxin oxidoreductase, or benzoylformate decarboxylase. Furthermore, addition of excess TDP had no effect on our observations, whereas it enhanced the regain of activity by benzoylformate decarboxylase when treated with [*p*-(bromomethyl)benzoyl]formic acid.<sup>6</sup> This reflects the stronger binding of the coenzyme by PDC compared to benzoylformate decarboxylase.

These conjugated pyruvic acid analogues have become useful in metabolic studies as well. In a recent report (*E*)-4-(4-chlorophenyl)-2-oxo-3-butenic acid proved to be the most efficient reagent to demonstrate the participation of pyruvic acid in the

formation of *N*<sup>6</sup>-acetyl-*N*<sup>6</sup>-hydroxylysine.<sup>13</sup>

**Acknowledgment.** We gratefully acknowledge the donors of the Petroleum Research Fund, administered by the American Chemical Society, for support, the financial support of NSF-DMB 87-09758 and the Rutgers University Busch Fund, and the elemental analyses performed by Dr. Franz Scheidl at Hoffmann-La Roche Inc. (Nutley, NJ). Richard Paris benefited from an REU supplement to the NSF grant. Ms. Tina Zecca performed some of the early inhibition studies. Finally, we are grateful to the Anheuser Busch Brewing Co. (Newark, NJ), for their continued generosity in supplying the live brewers' yeast.

(13) Szcapan, E. W.; Kaller, D.; Honek, J. F.; Viswanatha, T. *FEBS Lett.* 1987, 211, 239.

## Voltammetric Studies of the Interaction of Metal Chelates with DNA. 2. Tris-Chelated Complexes of Cobalt(III) and Iron(II) with 1,10-Phenanthroline and 2,2'-Bipyridine

Michael T. Carter, Marisol Rodriguez, and Allen J. Bard\*

Contribution from the Department of Chemistry, The University of Texas at Austin, Austin, Texas 78712. Received April 24, 1989

**Abstract:** Voltammetric methods were used to probe the interaction (electrostatic or intercalative) of metal complexes,  $ML_3^{3+/2+}$  ( $M = Fe, Co; L = 1,10\text{-phenanthroline}, 2,2'\text{-bipyridine}$ ), with calf thymus DNA. Binding constants ( $K_{n+}$ ) and binding site sizes ( $s$ ) were determined from voltammetric data, i.e., shifts in potential and changes in limiting current with addition of DNA. The exact magnitude for the parameters depends on whether the  $ML_3^{3+/2+}/DNA$  reaction is assumed to be static (S) or mobile (M) within the characteristic time of a voltammetric experiment.  $Co(phen)_3^{3+/2+}$  binds via intercalation with  $K_{3+} = 1.6 (\pm 0.2) \times 10^4 M^{-1}$  (S,  $s = 6$  bp) to  $2.6 (\pm 0.4) \times 10^4 M^{-1}$  (M,  $s = 5$  bp). The 2+ ion interacts more favorably via hydrophobic interaction with the nucleotide bases than does the 3+ ion. Both forms of the  $Fe(phen)_3^{2+/3+}$  couple bind with approximately the same affinity,  $K_{2+} = 7.1 (\pm 0.2) \times 10^3 M^{-1}$  (S,  $s = 5$  bp) and  $1.47 (\pm 0.04) \times 10^4 M^{-1}$  (M,  $s = 4$  bp).  $Co(bpy)_3^{3+/2+}$  shows appreciable electrostatic binding in 50 mM NaCl solution [ $K_{3+} = 9.4 (\pm 1.5) \times 10^3 M^{-1}$  (S) to  $1.4 (\pm 0.3) \times 10^4 M^{-1}$  (M),  $s = 3$  bp in each case], whereas  $Fe(bpy)_3^{2+/3+}$  does not bind at these ionic strengths. At lower ionic strength (10 mM NaCl, 10 mM Tris, pH 7.1), binding of  $Fe(bpy)_3^{2+/3+}$  is enhanced [ $K_{2+} = 1.1 (\pm 0.6) \times 10^3 M^{-1}$  nS,  $s = 4$  bp) to  $1.4 (\pm 0.1) \times 10^3 M^{-1}$  (M,  $s = 3$  bp)].

We describe here voltammetric studies of the interaction of the coordination complexes  $Co(bpy)_3^{3+}$ ,  $Fe(bpy)_3^{2+}$  (bpy = 2,2'-bipyridyl),  $Co(phen)_3^{3+}$ , and  $Fe(phen)_3^{2+}$  (phen = 1,10-phenanthroline) with calf thymus DNA. We extend our previously reported studies of  $Co(phen)_3^{3+}$ -DNA interactions via electrochemical methods<sup>1</sup> and describe the dependence of the electrochemical behavior on the nature of the ligands coordinated to the metal center.

A number of metal chelates have been used as probes of DNA structure, in solution,<sup>2</sup> as agents for mediation of strand scission of duplex DNA,<sup>3</sup> and as chemotherapeutic agents.<sup>4</sup> Ruthenium(II) complexes with phen and related ligands have been studied

extensively as structural probes<sup>5</sup> and mediators of DNA cleavage reactions.<sup>6</sup> Enantioselective interactions of phen and bpy complexes of iron(II) have also been used as structural probes,<sup>7</sup> and Fe(II) chelated by EDTA<sup>8</sup> and other complexing agents,<sup>9</sup> tethered

- (1) Carter, M. T.; Bard, A. J. *J. Am. Chem. Soc.* 1987, 109, 7528.  
 (2) (a) Barton, J. K. *J. Biomol. Struct. Dyn.* 1983, 1, 621. (b) Neidle, S.; Abraham, Z. *CRC Crit. Rev. Biochem.* 1984, 17, 73. (c) Dougherty, G.; Pilbrow, J. R. *Int. J. Biochem.* 1984, 16, 1179. (d) Barton, J. K. *Commun. Inorg. Chem.* 1985, 3, 321. (e) Barton, J. K. *Science* 1986, 233, 727.  
 (3) (a) Dervan, P. B. *Science* 1986, 232, 464. (b) Sigman, D. S. *Acc. Chem. Res.* 1986, 19, 180. (c) Schultz, P. G.; Dervan, P. B. *J. Biomol. Struct. Dyn.* 1984, 1, 1133.  
 (4) (a) Lippard, S. J. *Acc. Chem. Res.* 1978, 11, 211. (b) Roberts, J. J.; Thomson, A. J. *Prog. Nucleic Acid Res. Mol. Biol.* 1979, 22, 71. (c) Dabrowiak, J. C. in *Advances in Inorganic Biochemistry*; Eichhorn, G. L.; Marzilli, L. G., Eds.; Elsevier Biomedical: New York, 1982; Vol. 4, pp 69-113. (d) Hecht, S. M. *Acc. Chem. Res.* 1986, 19, 383. (e) Reedijk, J. *Pure Appl. Chem.* 1987, 59, 181.

- (5) (a) Barton, J. K.; Danishefsky, A. T.; Goldberg, J. M. *J. Am. Chem. Soc.* 1984, 106, 2172. (b) Barton, J. K.; Basile, L. A.; Danishefsky, A. T.; Alexandrescu, A. *Proc. Natl. Acad. U.S.A.* 1984, 81, 1961. (c) Kelley, J. M.; Tossi, A. B.; McConnell, D. J.; OhUigin, C. *Nucleic Acids Res.* 1985, 13, 6017. (d) Barton, J. K.; Lolis, E. *J. Am. Chem. Soc.* 1985, 107, 708. (e) Kumar, C. V.; Barton, J. K.; Turro, N. J. *J. Am. Chem. Soc.* 1985, 107, 5518. (f) Mei, H.-Y.; Barton, J. K. *J. Am. Chem. Soc.* 1986, 108, 7414. (g) Barton, J. K.; Goldberg, B. M.; Kumar, C. V.; Turro, N. J. *J. Am. Chem. Soc.* 1986, 108, 2081. (h) Goldstein, B. M.; Barton, J. K.; Berman, H. M. *Inorg. Chem.* 1986, 25, 842. (i) Stradowski, C.; Görner, H.; Currell, L. J.; Schulte-Frohlinde, D. *Biopolymers* 1987, 26, 189.  
 (6) (a) Basile, L. A.; Barton, J. K. *J. Am. Chem. Soc.* 1987, 109, 7548. (b) Basile, L. A.; Raphael, A. L.; Barton, J. K. *J. Am. Chem. Soc.* 1987, 109, 7550.  
 (7) Härd, T.; Nordén, B. *Biopolymers* 1986, 25, 1209.  
 (8) (a) Schultz, P. G.; Taylor, J. S.; Dervan, P. B. *J. Am. Chem. Soc.* 1982, 104, 6861. (b) Schultz, P. G.; Dervan, P. B. *Proc. Natl. Acad. Sci. U.S.A.* 1983, 80, 6834. (c) Taylor, J. S.; Schultz, P. G.; Dervan, P. B. *Tetrahedron* 1984, 40, 457. (d) Youngquist, R. S.; Dervan, P. B. *J. Am. Chem. Soc.* 1985, 107, 5528. (e) Dreyer, G. B.; Dervan, P. B. *Proc. Natl. Acad. Sci. U.S.A.* 1985, 82, 968. (f) Youngquist, R. S.; Dervan, P. B. *Proc. Natl. Acad. Sci. U.S.A.* 1985, 82, 2565. (g) Griffin, J. H.; Dervan, P. B. *J. Am. Chem. Soc.* 1987, 109, 6840. (h) Schultz, P. G.; Dervan, P. B. *J. Am. Chem. Soc.* 1983, 105, 7748.

to a second moiety which interacts with duplex DNA by intercalation and/or groove binding, have been intensively studied in the photoactivated cleavage of DNA. Enantioselective binding and DNA strand scission have also been reported for metallointercalation systems based on Pt(II),<sup>10a-f</sup> Zn(II),<sup>10g</sup> Cu(II), and Cu(I).<sup>11,12</sup> We have chosen to concentrate this work on complexes of Co(III) and Fe(II), which have not received as much attention as the Ru(II) systems but possess the same interesting characteristics of metallointercalation and DNA cleaving properties.<sup>13,14</sup> The electrochemical behavior of the bpy and phen complexes of Co(III)/(II) and Fe(II)/(III) are well-understood,<sup>15</sup> providing well-behaved systems for the study of the interactions of these species with DNA, via electrochemical methods.

The application of electrochemical methods to the study of metallointercalation and coordination of metal ions and chelates to DNA provides a useful complement to the previously used methods of investigation, such as UV-visible spectroscopy. Small molecules which are not amenable to such methods, either because of weak absorption bands or because of overlap of electronic transitions with those of the DNA molecule, can potentially be studied via voltammetric techniques. Multiple oxidation states of the same species as well as mixtures of several interacting species can be observed simultaneously. Equilibrium constants (*K*) for the interaction of the metal complexes with DNA can be obtained from shifts in peak potentials, and the number of base pair sites involved in binding (*s*) via intercalative, electrostatic, or hydrophobic interactions can be obtained from the dependence of the current passed during oxidation or reduction of the bound species on the amount of added DNA. In some cases it should also be possible to obtain kinetic data from current and potential measurements, since voltammetric methods are sensitive to chemical reactions (e.g., ligand dissociation) coupled to the electron-transfer steps.

A number of studies have addressed the electrochemistry of DNA, via redox reactions of the purine and pyrimidine bases.<sup>16</sup>

However, compared to spectroscopic methods, electrochemical methods have received little attention for studies of the interaction of small molecules with DNA. Several anthracycline antibiotics, which bind to DNA via intercalative and electrostatic interactions with the sugar-phosphate backbone,<sup>17</sup> have been studied electrochemically, as have the intercalating dyes methylene blue, neutral red, and cresyl violet.<sup>18</sup> Osmium tetroxide has been examined as a polarographic marker for single-stranded DNA.<sup>19</sup> Binding of *cis*-dichlorodiammineplatinum(II) (*cis*-DDP) to DNA was analyzed via polarographic determination of the free *cis*-DDP, following reaction with DNA.<sup>20</sup> The adduct (NH<sub>3</sub>)<sub>2</sub>Ru<sup>III</sup>-DNA was examined in the single-stranded form by differential pulse voltammetry,<sup>21</sup> and the binding of aquo ions of Cu<sup>2+</sup> and Cd<sup>2+</sup> was investigated by polarographic methods.<sup>22</sup> However, while some of these earlier studies described measurements of *K* and *s*, they did not consider either diffusion of an equilibrium mixture of free and bound electroactive species or the effects of binding to DNA on the thermodynamics of electron transfer.

In this paper, we describe the application of electrochemical measurements of the redox couples Co(phen)<sub>3</sub><sup>3+/2+</sup>, Fe(phen)<sub>3</sub><sup>2+/3+</sup>, Co(bpy)<sub>3</sub><sup>3+/2+</sup>, and Fe(bpy)<sub>3</sub><sup>2+/3+</sup> in the presence of DNA to quantify the binding of the metal complexes to double-stranded DNA. Binding is interpreted in terms of the interplay of electrostatic interactions with the charged sugar-phosphate backbone and intercalative (hydrophobic) interactions within the DNA helix (i.e., the stacked base pairs).

## Experimental Section

**Materials.** Calf thymus DNA was obtained from Sigma Chemical Co. (St. Louis, MO) and used as received. The solid Na<sup>+</sup> salt was stored at 4 °C. Solutions of DNA (ca. 10<sup>-5</sup> M in nucleotide phosphate, NP) in 50 mM NaCl/5 mM Tris, pH 7.1, gave ratios of UV absorbance at 260 and 280 nm, *A*<sub>260</sub>/*A*<sub>280</sub>, of ca. 1.8–1.9, indicating that the DNA was sufficiently free of protein.<sup>23</sup> Subjecting the DNA to phenol extraction<sup>24</sup> failed to improve the value of *A*<sub>260</sub>/*A*<sub>280</sub>. Furthermore, cyclic voltammetry of concentrated DNA solutions (ca. 5.0 mM NP) at a hanging mercury drop electrode (PAR Model 303 static mercury drop electrode) failed to exhibit any faradaic processes at potentials between 0.0 and -1.0 V vs saturated calomel electrode (SCE) but showed a 10%–15% reduction in charging current, compared to that of the DNA-free supporting electrolyte. Significant contamination of the DNA solution by protein would be apparent in CV experiments, due to faradaic processes arising from reduction of Hg-S bonds formed upon adsorption of proteins, possessing sulfur-containing amino acids, to the Hg drop.<sup>25</sup> Several of the known histones which may be expected to be contaminants of calf thymus DNA contain electroactive -SH groups or disulfide bonds.<sup>26</sup> Concentrated stock solutions of DNA (5.0–12.0 mM NP) were prepared in the supporting electrolyte of interest, and concentrations were deter-

(9) (a) Sauville, E. A.; Stein, R. W.; Peisach, J.; Horwitz, S. B. *Biochemistry* **1978**, *17*, 2746. (b) Eliot, H.; Gianni, L.; Meyers, C. *Biochemistry* **1984**, *23*, 928. (c) McGall, G. H.; Rabow, L. E.; Stubbe, J.; Kozarich, J. W. *J. Am. Chem. Soc.* **1987**, *109*, 2836. (d) Gold, B.; Dange, V.; Moore, M. A.; Eastman, A.; van der Marel, G. A.; van Boom, J. H.; Hecht, S. M. *J. Am. Chem. Soc.* **1988**, *110*, 2347. (e) Sausville, E. A.; Peisach, J.; Horwitz, S. B. *Biochemistry* **1978**, *17*, 2740.

(10) (a) Jennette, K. W.; Lippard, S. J.; Vassiliades, G. A.; Bauer, W. R. *Proc. Natl. Acad. U.S.A.* **1974**, *71*, 3839. (b) Lippard, S. J.; Bond, P. J.; Wu, K. C.; Bauer, W. R. *Science* **1976**, *194*, 726. (c) Wang, A. H. J.; Nathans, J.; van der Marel, G.; van Boom, J. H.; Rich, A. *Nature* **1978**, *276*, 471. (d) Barton, J. K.; Lippard, S. J. *Biochemistry* **1979**, *18*, 2661. (e) Bowler, B. E.; Hollis, L. S.; Lippard, S. J. *J. Am. Chem. Soc.* **1984**, *106*, 6102. (f) McFadyen, W. D.; Wakelin, L. P. G.; Roos, I. A. G. *Biochem. J.* **1987**, *242*, 117. (g) Barton, J. K.; Dannenberg, J. J.; Raphael, A. L. *J. Am. Chem. Soc.* **1982**, *104*, 4967.

(11) (a) Sigman, D. S.; Graham, D. R.; D'Aurora, V.; Stern, A. M. *J. Biol. Chem.* **1979**, *254*, 12269. (b) Que, B. G.; Downey, K. M.; So, A. G. *Biochemistry* **1980**, *19*, 5987. (c) Marshall, L. E.; Graham, D. R.; Reich, K. A.; Sigman, D. S. *Biochemistry* **1981**, *20*, 244. (d) Reich, K. A.; Marshall, L. E.; Graham, D. R.; Sigman, D. S. *J. Am. Chem. Soc.* **1981**, *103*, 3582. (e) Gutteridge, J. M. C.; Halliwell, B. *Biochem. Pharmacol.* **1982**, *31*, 2801. (f) Goldstein, S.; Czapski, G. *J. Am. Chem. Soc.* **1986**, *108*, 224. (g) Goynes, T. E.; Sigman, D. S. *J. Am. Chem. Soc.* **1987**, *109*, 2846.

(12) (a) Kuwahara, J.; Suzuki, T.; Funakoshi, K.; Sugiura, Y. *Biochemistry* **1986**, *25*, 1216. (b) Chen, C.-H.; Sigman, D. S. *Science* **1987**, *237*, 1197. (c) Ehrenfield, G. M.; Shipley, J. B.; Heimbrook, D. C.; Sugiyama, H.; Long, E. C.; van Boom, J. H.; van der Marel, G. A.; Oppenheimer, N. J.; Hecht, S. M. *Biochemistry* **1987**, *26*, 931.

(13) (a) Barton, J. K.; Raphael, A. L. *J. Am. Chem. Soc.* **1984**, *106*, 2466. (b) Barton, J. K.; Raphael, A. L. *Proc. Natl. Acad. U.S.A.* **1985**, *82*, 6460. (c) Barton, J. K.; Paranawithana, S. R. *Biochemistry* **1986**, *25*, 2205.

(14) (a) Chang, C.-H.; Meares, C. F. *Biochemistry* **1982**, *21*, 6332. (b) Subramanian, R.; Meares, C. F. *J. Am. Chem. Soc.* **1986**, *108*, 6427.

(15) (a) Maki, N.; Tanaka, N. In *Encyclopedia of Electrochemistry of The Elements*; Bard, A. J., Ed.; Marcel Dekker: New York, 1975; Vol. 3, pp 43–210 and references cited therein. (b) Heusler, K. E. *Ibid.*, Vol. 9, pp 230–381 and references cited therein.

(16) (a) Séquaris, J.-M.; Kaba, M. L.; Valenta, P. *Bioelectrochem. Bioenerg.* **1984**, *13*, 225. (b) Berg, H. In *Comprehensive Treatise of Electrochemistry*; Srinivasan, S.; Chizmadzhev, Y. A.; Bockris, J. O'M.; Conway, B. E., Eds.; Plenum Press: New York, 1985; Vol. 10, Chapter 3. (c) Berg, H.; Fiedler, U.; Flemming, J.; Horn, G. *Bioelectrochem. Bioenerg.* **1985**, *14*, 417. (d) Paleček, E.; Jelen, F.; Trnková, L. *Gen. Physiol. Biophys.* **1986**, *5*, 315. (e) Declercq, P. J.; De Ranter, C. *J. Chem. Soc. Faraday Trans. 1* **1987**, *83*, 257. (f) Paleček, E. *Bioelectrochem. Bioenerg.* **1986**, *15*, 275. (g) Paleček, E.; Lukášová, E.; Jelen, F.; Vojtišková, M. *Bioelectrochem. Bioenerg.* **1981**, *8*, 497. (h) Séquaris, J.-M.; Valenta, P. *J. Electroanal. Chem.* **1987**, *227*, 11.

(17) (a) Calendi, E.; Di Marco, A.; Reggiani, M.; Scarpinato, B.; Valenti, L. *Biochim. Biophys. Acta* **1965**, *103*, 25. (b) Berg, H.; Horn, G.; Luthardt, U.; Ihn, W. *Bioelectrochem. Bioenerg.* **1981**, *8*, 537. (c) Molinier-Jumel, C.; Malfroy, B.; Reynaud, J. A.; Aubeil-Sadron, G. *Biochem. Biophys. Res. Commun.* **1978**, *84*, 441.

(18) Kelley, J. M.; Lyons, M. E. G.; Van Der Putten, W. J. M. In *Electrochemistry, Sensors and Analysis*; Smyth, M. R.; Vos, J. G., Eds.; Analytical Chemistry Symposium Series; Elsevier: Amsterdam, 1986; Vol. 25, p 205.

(19) Paleček, E.; Vojtišková, M.; Jelen, F.; Lukášová, E. *Bioelectrochem. Bioenerg.* **1984**, *12*, 135.

(20) Vrána, O.; Brabec, V. *Anal. Biochem.* **1984**, *142*, 16.

(21) Clarke, M. J.; Jansen, B.; Marx, K. A.; Kruger, R. *Inorg. Chim. Acta* **1986**, *124*, 13.

(22) Bach, D.; Miller, I. R. *Biopolymers* **1967**, *5*, 161.

(23) Marmur, J. *J. Mol. Biol.* **1961**, *3*, 208.

(24) Maniatis, T.; Fritsch, E. F.; Sambrook, J. *Molecular Cloning*; Cold Spring Harbor Laboratory: Cold Spring Harbor, NY, 1982.

(25) (a) Stankovich, M. T.; Bard, A. J. *J. Electroanal. Chem.* **1978**, *86*, 189. (b) Stankovich, M. T.; Bard, A. J. *J. Electroanal. Chem.* **1977**, *85*, 173.

(26) Craft, L. R. *Handbook of Protein Sequence Analysis*, 2nd ed.; Wiley: Chichester, 1980; pp 459–466 and references cited therein.

**Table I.** Voltammetric Behavior of  $\text{Co(phen)}_3^{3+/2+}$  in the Presence of DNA<sup>a</sup>

$\nu/\text{V}\cdot\text{s}^{-1}$	$R^b$	$E_{pc}/\text{V}^c$	$E_{pa}/\text{V}$	$\Delta E_p/\text{mV}$	$E_{1/2}/\text{V}$	$i_{pa}/i_{pc}$	$i_{pc}/i_{pc} (R = 0)$
0.01	0	0.107 (1)	0.172 (2)	65	0.140	1.05	1
	30	0.122 (2)	0.180 (4)	58	0.151	1.05	0.46
	50	0.122 (3)	0.183 (2)	61	0.153	1.1	0.34
	70	0.123 (2)	0.187 (3)	64	0.155	0.97	0.32
0.10	0	0.107 (1)	0.173 (2)	66	0.140	1.15	1
	30	0.122 (1)	0.180 (2)	58	0.151	1.0	0.52
	50	0.122 (2)	0.182 (1)	60	0.152	0.99	0.41
	70	0.120 (2)	0.182 (1)	62	0.151	0.87	0.39
1.0	0	0.110 (3)	0.179 (2)	68	0.145	1.17	1
	30	0.124 (2)	0.183 (2)	59	0.154	1.09	0.54
	50	0.116 (5)	0.187 (4)	71	0.152	0.95	0.44
	70	0.099 (4)	0.181 (3)	82	0.140	0.72	0.47

<sup>a</sup>Supporting electrolyte, 50 mM NaCl + 5 mM Tris, pH 7.1. <sup>b</sup> $[\text{Co(phen)}_3^{3+}] = 1.0 \times 10^{-4}$  M. <sup>c</sup>Numbers in parentheses are standard deviations for five measurements.

**Table II.** Voltammetric Behavior of  $\text{Fe(phen)}_3^{2+/3+}$  in the Presence of DNA<sup>a</sup>

$\nu/\text{V}\cdot\text{s}^{-1}$	$R^b$	$E_{pc}/\text{V}^c$	$E_{pa}/\text{V}$	$\Delta E_p/\text{mV}$	$E_{1/2}/\text{V}$	$i_{pa}/i_{pc}$	$i_{pc}/i_{pc} (R = 0)$
0.05	0	0.830 (1)	0.895 (1)	65	0.862	0.8	1
	39	0.829 (1)	0.902 (3)	73	0.865	0.7	0.52
	69	0.825 (1)	0.900 (3)	75	0.863	0.6	0.44
0.10	0	0.833 (3)	0.898 (4)	65	0.865	0.8	1
	39	0.828 (2)	0.904 (1)	76	0.866	0.7	0.51
	69	0.827 (1)	0.902 (1)	75	0.864	0.7	0.44
0.5	0	0.835 (1)	0.900 (5)	65	0.867	0.7	1
	39	0.835 (1)	0.898 (1)	63	0.866	0.7	0.48
	69	0.835 (1)	0.902 (3)	67	0.868	0.7	0.39

<sup>a</sup>Supporting electrolyte, 50 mM NaCl + 5 mM Tris, pH 7.1. <sup>b</sup> $[\text{Fe(phen)}_3^{2+}] = 8.0 \times 10^{-5}$  M. <sup>c</sup>Numbers in parentheses are standard deviations for five measurements.

mined by UV absorbance at 260 nm, on 1:100 dilutions. The extinction coefficient,  $\epsilon_{260}$ , was taken as  $6600 \text{ M}^{-1} \text{ cm}^{-1}$ .<sup>27</sup> Stock solutions were stored at 4 °C and discarded after no more than 4 days, unless treated with one or two drops of  $\text{CHCl}_3$ , which prolonged the useful life of DNA solutions for up to 7–10 days. The presence of  $\text{CHCl}_3$  had no effect on voltammetric results.

Tris(1,10-phenanthroline)cobalt(III) perchlorate trihydrate  $[\text{Co(phen)}_3(\text{ClO}_4)_3 \cdot 3\text{H}_2\text{O}]$ , tris(2,2'-bipyridyl)cobalt(III) perchlorate trihydrate  $[\text{Co(bpy)}_3(\text{ClO}_4)_3 \cdot 3\text{H}_2\text{O}]$ , tris(1,10-phenanthroline)iron(II) perchlorate  $[\text{Fe(phen)}_3(\text{ClO}_4)_2]$ , and tris(2,2'-bipyridyl)iron(II) dichloride  $[\text{Fe(bpy)}_3\text{Cl}_2]$  were prepared according to previously reported procedures.<sup>28</sup> Starting materials, 1,10-phenanthroline monohydrate (phen), 2,2'-bipyridine (bpy),  $\text{CoCl}_2 \cdot 6\text{H}_2\text{O}$ , and  $\text{FeSO}_4$ , were purchased from Aldrich Chemical Co. (Milwaukee, WI) and used as received. The complexes were recrystallized twice from water and dried overnight, under vacuum, at 25 °C. Stock solutions of the metal complexes were prepared before each series of experiments and were discarded afterward.

Potassium octacyanomolybdate(IV) dihydrate  $[\text{K}_4\text{Mo(CN)}_8 \cdot 2\text{H}_2\text{O}]$  was prepared as described previously.<sup>29</sup> Potassium ferricyanide  $[\text{K}_3\text{Fe(CN)}_6]$ , was purchased from Aldrich and used without further purification.

All other chemicals used for preparation of supporting electrolytes (NaCl, Tris, HCl) were reagent grade. Solutions were prepared in high-purity water ( $\rho = 18 \text{ M}\Omega\cdot\text{cm}$ ) from a Millipore Milli-Q water purification system.

**Instrumentation.** Cyclic voltammetry (CV) was performed with a Bioanalytical Systems (West Lafayette, IN) Model BAS-100 electrochemical analyzer or with a Princeton Applied Research (PAR) Model 173 potentiostat/175 universal programmer with data storage and manipulation via a Norland Corp. (Fort Atkinson, WI) Model 3001 digital oscilloscope. Differential pulse voltammetry (DPV) and chronocoulometry (CC) employed the BAS-100 electrochemical analyzer, with the following parameters (DPV): pulse amplitude = -50 mV, pulse width = 50 ms, sweep rate ( $\nu$ ) = 4 mV/s, and pulse period = 1 s. Typically, CV peak potentials were reproducible to better than  $\pm 5$  mV (at moderate sweep rates) and DPV peak potentials to  $\pm 2$  mV. Cell resistances were measured with a Yellow Springs Instruments Model 35 conductance meter. Ultraviolet-visible spectra were obtained on a Hewlett-Packard Model 8450A spectrophotometer.

(27) Reichmann, M. E.; Rice, S. A.; Thomas, C. A.; Doty, P. *J. Am. Chem. Soc.* **1954**, *76*, 3047.

(28) (a) Dollimore, L. S.; Gillard, R. D. *J. Chem. Soc., Dalton Trans.* **1973**, 933. (b) Musumeci, S.; Rizzarelli, F. S.; Sammartano, S.; Bonomo, R. P. *Inorg. Chim. Acta* **1973**, *7*, 660. (c) Gaudello, J. G.; Sharp, P. R.; Bard, A. J. *J. Am. Chem. Soc.* **1982**, *104*, 6373.

(29) Furman, N. H.; Miller, C. O. *Inorg. Synth.* **1950**, *3*, 160.

**Procedures.** All voltammetric experiments were performed in single-compartment cells of volume 5–15 mL. The working electrodes were glassy carbon disks (Bioanalytical Systems, West Lafayette, IN) with a geometric area of  $0.071 \text{ cm}^2$  [for  $\text{Co(III)/(II)}$  systems] or  $0.088 \text{ cm}^2$  [for  $\text{Fe(II)/(III)}$  systems]. The working electrode was polished prior to each series of experiments with  $0.25\text{-}\mu\text{m}$  diamond paste (Buehler, Lake Bluff, IL) on a nylon buffing pad and then subjected to ultrasonic cleaning for ca. 5 min, in 95% ethanol. The use of  $0.05\text{-}\mu\text{m}$  alumina, in place of diamond paste, proved unsatisfactory. Erratic peak potentials were obtained in CV of  $\text{Co(III)/(II)}$  redox couples under these conditions, as well as some irreproducibility in current measurement. A saturated calomel electrode (SCE), prepared according to Adams,<sup>30</sup> was used in all experiments. A Pt flag served as counter electrode.

Supporting electrolytes were 50 mM NaCl/5 mM Tris (denoted buffer 1) or 10 mM NaCl/10 mM Tris (denoted buffer 2), adjusted to pH 7.1 with HCl. Assembled cells had a resistance (working electrode to counter electrode) of  $500 \Omega$  (buffer 1) and  $770 \Omega$  (buffer 2). Thus, the maximum distortion in peak potential, due to IR drop, was 2 mV (in buffer 1) and 3 mV (in buffer 2) at the maximum currents passed during voltammetric experiments (ca.  $3.5 \mu\text{A}$ ).

All glassware for solution preparation and electrochemical experiments was silanized with a 5% (v/v) solution of trimethylchlorosilane (Petrarch Systems, Bristol, PA) in toluene. Where appropriate, solutions were deoxygenated via purging with  $\text{N}_2$  gas for 15 min prior to measurements; during measurements, a stream of  $\text{N}_2$  was passed over the solution.  $\text{N}_2$  was passed through an  $\text{O}_2$  scrubbing system<sup>31</sup> and saturated with the aqueous supporting electrolyte before entering the electrochemical cell.

Nonlinear regression analysis of titration data, presented below, was performed with SAS statistical software (The SAS Institute, Inc., Cary, NC) on an IBM 3081D computer system.

All experiments were carried out at the ambient temperature of the laboratory (23–25 °C). All measurements, unless specified otherwise, are the average of at least three to five replicate measurements.

## Results

**$\text{Co(phen)}_3^{3+/2+}$  and  $\text{Fe(phen)}_3^{3+/2+}$ .** Typical CV behavior of 0.10 mM  $\text{Co(phen)}_3^{3+}$  in the absence and presence of DNA is shown in Figure 1 and that of 0.076 mM  $\text{Fe(phen)}_3^{2+}$ , under similar conditions, in Figure 2. Summaries of voltammetric results are given in Tables I and II. The supporting electrolyte for all experiments was buffer 1. CV of  $\text{Co(phen)}_3^{3+/2+}$  ( $\nu = 100 \text{ mV/s}$ ) in the absence of DNA (Figure 1A) featured reduction of 3+ to

(30) Adams, R. N. *Electrochemistry at Solid Electrodes*; Marcel Dekker: New York, 1969; pp 288–291.

(31) Rusling, J. F. *J. Electroanal. Chem.* **1981**, *125*, 447.

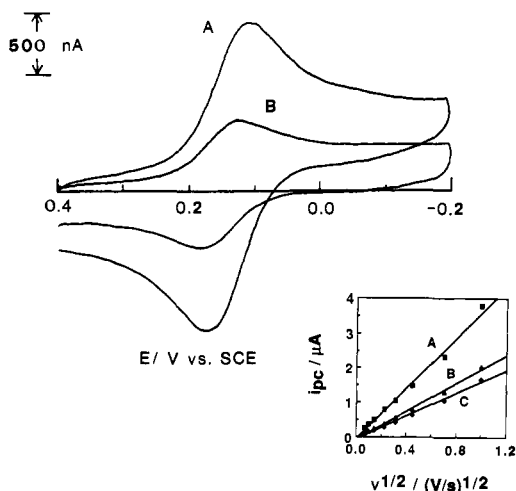


**Figure 1.** Cyclic voltammograms of  $1.0 \times 10^{-4}$  M  $\text{Co}(\text{phen})_3^{3+}$  in the (A) absence and (B) presence of 5.0 mM nucleotide phosphate (NP). Sweep rate, 100 mV/s. Supporting electrolyte, buffer 1. Inset: Effect of DNA on the diffusion of  $\text{Co}(\text{phen})_3^{3+}$  at (A)  $R = 0$ , (B)  $R = 30$ , and (C)  $R = 50$ .

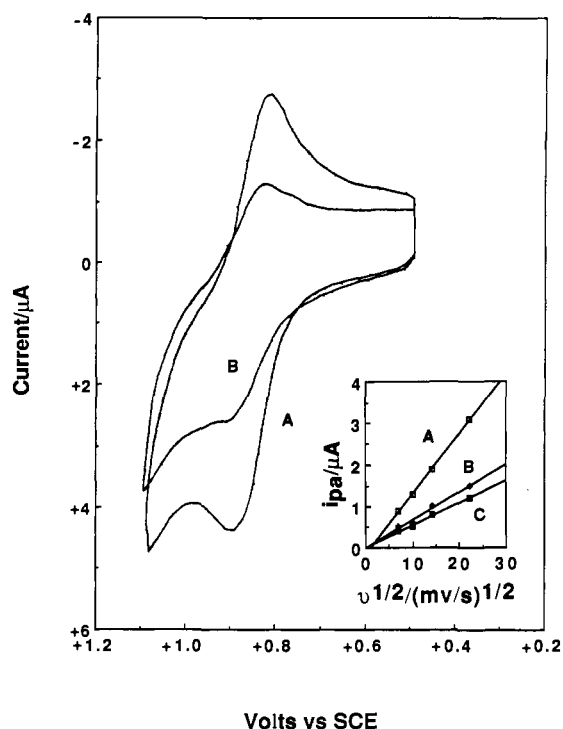


**Figure 2.** Cyclic voltammograms of  $7.6 \times 10^{-5}$  M  $\text{Fe}(\text{phen})_3^{2+}$  (A) in the absence and (B) presence of 3.39 mM NP. Supporting electrolyte, buffer 1. Sweep rate, 500 mV/s. Inset: Effect of DNA on the diffusion of  $\text{Fe}(\text{phen})_3^{2+}$  at (A)  $R = 0$ , (B)  $R = 41.2$ , and (C)  $R = 72.1$ .

the  $2+$  form at a cathodic peak potential,  $E_{pc}$ , of 0.107 V vs SCE. Reoxidation of  $2+$  occurred, upon scan reversal, at 0.174 V. The separation of the anodic and cathodic peak potentials,  $\Delta E_p$ , 67 mV, indicated a quasireversible,  $1-e^-$  redox process. The formal potential,  $E^\circ$  (or voltammetric  $E_{1/2}$ ), taken as the average of  $E_{pc}$  and  $E_{pa}$ , was 0.140 V, in the absence of DNA. In the presence of 5.0 mM nucleotide phosphate, NP (Figure 1B), at the same concentration of  $\text{Co}(\text{phen})_3^{3+}$ ,  $E_{pc} = 0.125$  V and  $E_{pa} = 0.183$  V. Thus, both the anodic and cathodic peak potentials shifted to more positive values vs a solution without DNA ( $E_{1/2} = 0.154$  V). The value of  $\Delta E_p$  in the presence of DNA was 58 mV, showing that reversibility of the electron-transfer process was maintained or even improved under these conditions.  $E_{1/2}$ , in this case, shifted to more positive potentials by 14 mV.

CV peak potentials were independent of sweep rate,  $\nu$ , over the range 5–1.0 V/s, with  $\Delta E_p$  in the range of 62–68 mV, in the

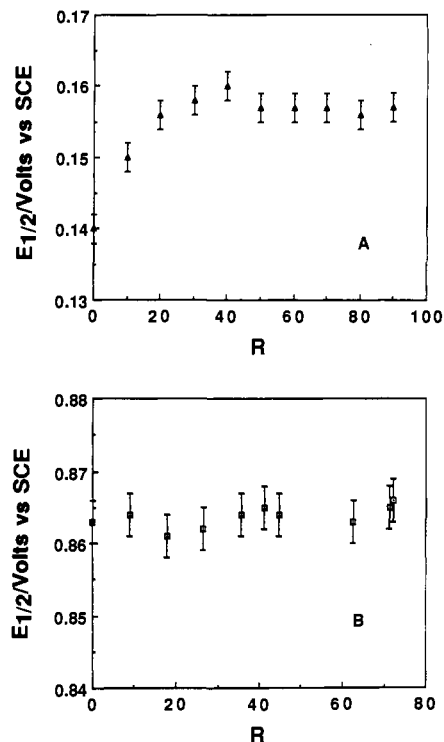


**Figure 3.** Dependence of  $E_{1/2}$  on the ratio NP:metal complex,  $R$ , for (A)  $1.0 \times 10^{-4}$  M  $\text{Co}(\text{phen})_3^{3+}$  (by DPV) and (B)  $7.6 \times 10^{-5}$  M  $\text{Fe}(\text{phen})_3^{2+}$  (by CV). Supporting electrolyte, buffer 1.

absence of DNA. In the presence of DNA ( $0 < \text{concentration of nucleotide phosphate, } [\text{NP}] \leq 7.0$  mM) and at intermediate  $\nu$  ( $5 \text{ mV/s} \leq \nu \leq 200 \text{ mV/s}$ ),  $\Delta E_p$  was somewhat smaller (58–61 mV) with  $E_{pc}$  and  $E_{pa}$  independent of  $\nu$ . At higher  $\nu$  and in the presence of DNA (e.g., 1.0 V/s), slight broadening of  $\Delta E_p$  was observed, possibly due to the onset of kinetic complications ( $\Delta E_p > 70$  mV) as well as a slight dependence of  $E_p$  on  $\nu$  (e.g.,  $E_{pc} = 0.123$  V at 0.01 V/s and  $[\text{NP}] = 7.0$  mM, while  $E_{pc} = 0.099$  V at 1.0 V/s and  $[\text{NP}] = 7.0$  mM).

Typical behavior of  $\text{Fe}(\text{phen})_3^{2+/3+}$  ( $\nu = 500$  mV/s) is shown in A and B of Figure 2 for a solution without DNA and in the presence of 3.4 mM NP, respectively. In the absence of DNA,  $\text{Fe}(\text{phen})_3^{2+}$  was oxidized to the  $3+$  ion at  $E_{pa} = 0.898$  V and reduced, upon scan reversal, at  $E_{pc} = 0.828$  V;  $E_{1/2} = 0.863$  V ( $\Delta E_p = 70$  mV). In the presence of DNA ( $R = 45$ ),  $E_{1/2}$  was 0.864 V and  $\Delta E_p$  was 68 mV. Reversibility of the electron transfer was maintained in the presence of DNA, but there was no apparent shift in  $E_{1/2}$ . Peak potentials were independent of scan rate ( $50 \leq \nu \leq 500$  mV/s), and  $\Delta E_p$  values were between 63 and 76 mV.

The positive shift in  $E_{1/2}$  with increasing ratio of total concentration of NP to total concentration of  $\text{Co}(\text{III})$ ,  $R$ , suggests a difference in the binding properties of the  $\text{Co}(\text{III})$  and  $\text{Co}(\text{II})$  species to DNA. The absence of a shift in  $E_{1/2}$  of the  $\text{Fe}(\text{II})/(\text{III})$  couple, however, suggests that the two halves of this redox couple interact with DNA to about the same extent. Figure 3 shows results for experiments in which the  $[\text{NP}]$  was varied over a wide range for 0.1 mM  $\text{Co}(\text{phen})_3^{3+}$  (Figure 3A) and 0.076 mM  $\text{Fe}(\text{phen})_3^{2+}$  (Figure 3B).  $E_{1/2}$  values were determined from the DPV peak potential (in Figure 3A),  $E_p$ , by the relation<sup>32a</sup>

$$E_{1/2} = E_p + \Delta E/2 \quad (1)$$

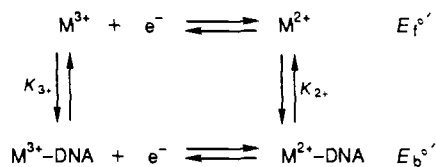
where  $E_{1/2}$  is the equivalent of the average of  $E_{pc}$  and  $E_{pa}$  in CV experiments and  $\Delta E$  is the pulse amplitude (–50 mV). These  $E_{1/2}$  values were in good agreement with those determined from CV experiments. The average of  $E_{pc}$  and  $E_{pa}$  was used to determine  $E_{1/2}$  in Figure 3B. The limiting shift in  $E_{1/2}$  of +17 mV for  $\text{Co}(\text{phen})_3^{3+}$  was taken as the difference between the  $E_{1/2}$  at  $R$

(32) Bard, A. J.; Faulkner, L. R. *Electrochemical Methods*; Wiley: New York, 1980; (a) p 194, (b) p 219.

**Table III.** Voltammetric Behavior of  $\text{Mo}(\text{CN})_8^{4-/3-}$  and  $\text{Co}(\text{phen})_3^{3+/2+}$  in the Presence of DNA<sup>a</sup>

couple	$R^b$	$E_{pc}/\text{V}$	$E_{pa}/\text{V}$	$E_{1/2}/\text{V}$	$\Delta E_p/\text{mV}$	$i_{pc}/\mu\text{A}$	$i_{pa}/\mu\text{A}$	$i_{pc}/i_{pc}(R=0)$	$i_{pa}/i_{pa}(R=0)$
Mo	0	0.560	0.482	0.521	78	0.4	1.02		1
	54.5	0.564	0.485	0.525	79	0.38	0.99		0.97
Co	0	0.104	0.170	0.137	66	1.3	1.1	1	
	54.5	0.115	0.183	0.149	68	0.6	0.4	0.36	

<sup>a</sup>Supporting electrolyte, 50 mM NaCl + 5 mM Tris, pH 7.1. Sweep rate, 100 mV/s. <sup>b</sup> $[\text{Co}(\text{phen})_3^{3+}] = 1.1 \times 10^{-4} \text{ M}$ ;  $[\text{Mo}(\text{CN})_8^{4-}] = 1.1 \times 10^{-4} \text{ M}$ .

**Scheme I**


= 0 and the average of the  $E_{1/2}$  values corresponding to the plateau of the  $E_{1/2}$ - $R$  curve ( $R \geq 30$ ).  $E_{1/2}$  for  $\text{Fe}(\text{phen})_3^{2+}$  did not change appreciably, over the same range of [NP].

The net shift in  $E_{1/2}$  can be used to estimate the ratio of equilibrium constants for the binding of the 3+ and 2+ ions to DNA. This is analogous to the treatment of the association of small molecules with micelles.<sup>33</sup> For a Nernstian electron transfer, in a system in which both the oxidized and reduced forms associate with a third species in solution (DNA), Scheme I can be applied. Here,  $\text{M}^{3+}$  and  $\text{M}^{2+}$  represent the oxidized and reduced forms of the metal complex and  $\text{M}^{n+}$ -DNA denotes a metal complex bound to the DNA molecule.  $E_f^{o'}$  and  $E_b^{o'}$  are the formal potentials of the 3+/2+ couple, in the free and bound forms, respectively.  $K_{3+}$  and  $K_{2+}$  are the corresponding binding constants for the 3+ and 2+ species to DNA. Consideration of the Nernst equations for the reversible redox reactions of the free and bound species and the corresponding equilibrium constants for binding of each oxidation state to DNA yields, for a 1- $e^-$  redox process

$$E_b^{o'} - E_f^{o'} = 0.059 \log (K_{2+}/K_{3+}) \quad (2)$$

Thus, for a limiting shift of +17 mV,  $K_{2+}/K_{3+}$  for  $\text{Co}(\text{phen})_3^{3+/2+}$  is 1.94; i.e., the 2+ ion is apparently bound about twice as strongly as the 3+ ion. However, in the case of  $\text{Fe}(\text{phen})_3^{2+/3+}$ ,  $K_{2+}/K_{3+} = 1$ , and each oxidation state interacts with DNA to the same extent. The implications of these results are discussed in a subsequent section.

Previously,<sup>1</sup> we reported  $K_{2+}/K_{3+}$  to be 4.8, corresponding to a shift in  $E_{1/2}$  of +40 mV, over the range  $0 \leq R \leq 300$ . However, we have observed that the apparent  $E_{1/2}$  of  $\text{Co}(\text{phen})_3^{3+/2+}$ , in the absence of DNA, depends on the concentration of electroactive species. Since different concentrations of  $\text{Co}(\text{phen})_3^{3+}$  were used in the previous study to gain access to a very large range of  $R$  values (0.10 mM for  $0 \leq R \leq 100$  and 0.01 mM for  $100 < R \leq 300$ ), ca. 15–20 mV of the previously reported potential shift can be attributed to a dependence of  $E_{1/2}$  on the concentration of  $\text{Co}(\text{phen})_3^{3+}$ . The remainder of the shift is accountable via binding to DNA, within the error of the measurement. Diffusion coefficients in the free and bound limits are comparable at different concentrations of  $\text{Co}(\text{phen})_3^{3+}$ , however, since the ratio  $i_p/C$  (where  $i_p$  is the DPV peak current and  $C$  is the total concentration of electroactive species) is essentially constant over the concentration range  $10^{-6} \text{ M} \leq C \leq 10^{-4} \text{ M}$ .

In addition to changes in formal potential upon addition of DNA, the voltammetric current decreases, as shown in the insets of Figures 1 and 2. For  $\text{Co}(\text{phen})_3^{3+}$  (inset of Figure 1) plots of cathodic peak current,  $i_{pc}$ , vs  $\nu^{1/2}$  were linear with  $y$  intercepts = 0, within the error of the measurement, as expected for reversible  $e^-$  transfer.<sup>32b</sup> The slope of the  $i_{pc}-\nu^{1/2}$  plot decreased with increasing  $R$ , indicating a reduction in the apparent diffusion coefficient of  $\text{Co}(\text{phen})_3^{3+}$  as [NP] increased. The slope of inset curve A of Figure 1 ( $R = 0$ ) gives the diffusion coefficient of the free  $\text{Co}(\text{phen})_3^{3+}$ ,  $D_f$ , of  $3.7 (\pm 0.6) \times 10^{-6} \text{ cm}^2/\text{s}$ . Curves B and

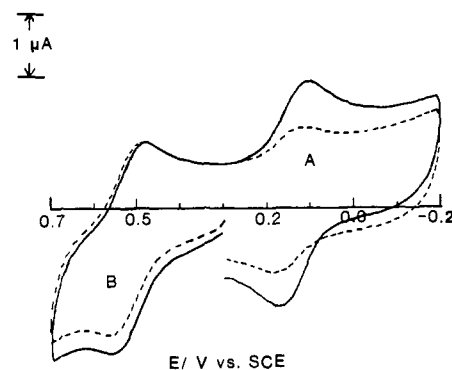


**Figure 4.** Cyclic voltammetry of a mixture of  $\text{Co}(\text{phen})_3^{3+}$  (redox couple A,  $1.1 \times 10^{-4} \text{ M}$ ) and  $\text{Mo}(\text{CN})_8^{4-}$  (redox couple B,  $1.1 \times 10^{-4} \text{ M}$ ), in the absence (solid curve) and the presence (dashed curve) of 5.45 mM NP. Sweep rate, 100 mV/s. Scan initiated at +0.30 V vs. SCE.

C correspond to apparent  $D$  values of  $1.14 \times 10^{-6} \text{ cm}^2/\text{s}$  ( $R = 30$ ) and  $7.5 \times 10^{-7} \text{ cm}^2/\text{s}$  ( $R = 50$ ), respectively. For  $\text{Fe}(\text{phen})_3^{2+}$  (see inset of Figure 2) similar measurements gave  $D_f = 4.9 (\pm 1) \times 10^{-6} \text{ cm}^2/\text{s}$ . In the limit of very large  $R$ , where binding of the metal complex to DNA is more nearly quantitative (see below), DPV measurements [ $R = 1000$ ,  $8.5 \times 10^{-6} \text{ M Co}(\text{phen})_3^{3+}$ ] gave a diffusion coefficient of the bound species,  $D_b$ , of  $2.6 (\pm 0.6) \times 10^{-7} \text{ cm}^2/\text{s}$ . Similar measurements on  $\text{Fe}(\text{phen})_3^{2+}$  ( $R = 1111$ ,  $1.0 \times 10^{-5} \text{ M}$  in complex) gave  $D_b = 9.0 (\pm 0.8) \times 10^{-8} \text{ cm}^2/\text{s}$ . Thus, the apparent diffusion coefficient of  $\text{Co}(\text{phen})_3^{3+}$  decreased by a factor of 14.2 and that of  $\text{Fe}(\text{phen})_3^{2+}$  by 55, upon addition of a large excess of DNA. These two experimental limits represent diffusion of the free and bound metal complex, respectively. In CV experiments at 0.1 mM Co(III),  $50 \leq R \leq 70$  ( $\nu = 100 \text{ mV/s}$ ), the value of  $i_{pc}$  was ca. 40% of that in the absence of DNA. The ratio of anodic to cathodic peak currents,  $i_{pa}/i_{pc}$ , was close to 1 under all experimental conditions, indicating that the 3+ and 2+ species are both stable on the time scale of the CV measurement. The ratio  $i_{pa}/i_{pc}$  was not affected by the presence of  $\text{O}_2$  in the solution, indicating that the 2+ ion was not reoxidized via dissolved  $\text{O}_2$  on the time scale of the experiment. For  $\text{Fe}(\text{phen})_3^{2+}$ ,  $i_{pa}$  decreased to ca. 43% of that in the absence of DNA, for solutions where  $40 \leq R \leq 70$ . The ratio  $i_{pa}/i_{pc}$  was 0.7–0.8 at all  $\nu$  and [NP].

We interpret the change in current upon DNA addition in terms of the diffusion of an equilibrium mixture of free and DNA-bound metal complex to the electrode surface. These changes can be used to quantify the binding of the metal complex to DNA and are addressed in more detail in a subsequent section.

**Effect of DNA on Diffusion of Anions.** To show that the decrease in  $i_{pc}$  is due to diffusion of the  $\text{M}(\text{phen})_3^{3+}$ -DNA adduct and not merely to diffusion of free metal complex in a solution of increased viscosity, nor to blockage of the electrode surface by an adsorbed layer of DNA that could possibly form at the electrode surface, experiments were carried out on a mixture of  $\text{Co}(\text{phen})_3^{3+}$  and  $\text{Mo}(\text{CN})_8^{4-}$ , at the same concentration (0.11 mM, in buffer 1), in the absence and presence of DNA ( $R = 54.5$ ), as shown in Figure 4. Results are summarized in Table III.  $\text{Mo}(\text{CN})_8^{4-}$  should not interact with DNA, because of coulombic repulsion between its high negative charge and the negatively charged sugar-phosphate backbone of DNA. In the absence of DNA (solid curve),  $\text{Mo}(\text{CN})_8^{4-/3-}$  (couple B) gave  $E_{1/2} = 0.521 \text{ V}$  and  $\text{Co}(\text{phen})_3^{3+/2+}$  (couple A) gave  $E_{1/2} = 0.137 \text{ V}$ . Upon addition of DNA (dashed curve),  $E_{1/2}$  for  $\text{Mo}(\text{CN})_8^{4-/3-}$  was 0.525 V and

**Table IV.** Voltammetric Behavior of  $\text{Co}(\text{bpy})_3^{3+/2+}$  in the Presence of DNA<sup>a</sup>

$\nu/\text{V}\cdot\text{s}^{-1}$	$R^b$	$E_{\text{pc}}/\text{V}^c$	$E_{\text{pa}}/\text{V}$	$\Delta E_{\text{p}}/\text{mV}$	$E_{1/2}/\text{V}$	$i_{\text{pa}}/i_{\text{pc}}$	$i_{\text{pc}}/i_{\text{pc}}(R=0)$
0.01	0	0.056 (3)	0.125 (3)	69	0.090	0.7	1
	30	0.052 (2)	0.118 (7)	66	0.085	0.56	0.57
	50	0.052 (1)	0.122 (5)	70	0.088	0.42	0.48
0.10	0	0.053 (1)	0.118 (1)	65	0.086	0.5	1
	30	0.040 (1)	0.105 (4)	65	0.073	0.24	0.7
	50	0.035 (1)	0.105 (3)	69	0.070	0.17	0.58
	70	0.035 (1)	0.109 (1)	74	0.072	0.17	0.56
1.0	0	0.027 (5)	0.110 (8)	83	0.069	0.41	1
	30	0.016 (2)	0.095 (1)	78	0.056	0.17	0.67
	50	-0.002 (5)	0.097 (2)	99	0.048	0.12	0.58

<sup>a</sup>Supporting electrolyte, 50 mM NaCl + 5 mM Tris, pH 7.1. <sup>b</sup> $[\text{Co}(\text{bpy})_3^{3+}] = 1.0 \times 10^{-4}$  M. <sup>c</sup>Numbers in parentheses are standard deviations for three measurements.

**Table V.** Voltammetric Behavior of  $\text{Fe}(\text{bpy})_3^{3+/2+}$  in the Presence of DNA<sup>a</sup>

$\nu/\text{V}\cdot\text{s}^{-1}$	$R^b$	$E_{\text{pc}}/\text{V}^c$	$E_{\text{pa}}/\text{V}$	$\Delta E_{\text{p}}/\text{mV}$	$E_{1/2}/\text{V}$	$i_{\text{pa}}/i_{\text{pc}}$	$i_{\text{pc}}/i_{\text{pc}}(R=0)$
0.05	0	0.822 (1)	0.887 (1)	65	0.856	0.9	1
	47	0.777 (1)	0.843 (1)	66	0.810	0.9	0.6
	66	0.783 (1)	0.845 (1)	62	0.814	0.8	0.51
0.10	0	0.822 (4)	0.884 (1)	62	0.853	0.8	1
	47	0.780 (1)	0.845 (1)	65	0.812	0.8	0.61
	66	0.781 (2)	0.847 (4)	66	0.814	0.9	0.52
0.5	0	0.820 (1)	0.892 (4)	72	0.855	0.9	1
	47	0.775 (1)	0.850 (1)	75	0.812	0.7	0.64
	66	0.775 (1)	0.850 (1)	75	0.812	0.9	0.48

<sup>a</sup>Supporting electrolyte, 10 mM NaCl + 10 mM Tris, pH 7.1. <sup>b</sup> $[\text{Fe}(\text{bpy})_3^{2+}] = 8.0 \times 10^{-5}$  M. <sup>c</sup>Numbers in parentheses are standard deviations for five measurements.

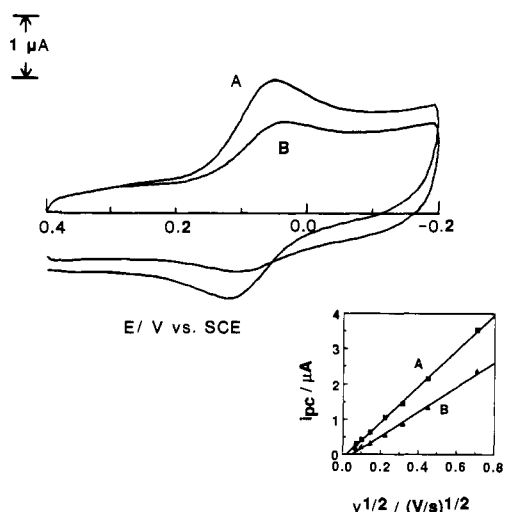


**Figure 5.** Cyclic voltammetry of  $1.0 \times 10^{-4}$  M  $\text{Co}(\text{bpy})_3^{3+}$  (A) in the absence and (B) in the presence of 5.0 mM NP. Inset: Effect of DNA on diffusion of  $\text{Co}(\text{bpy})_3^{3+}$ , at (A)  $R = 0$  and (B)  $R = 50$ . Supporting electrolyte, buffer 1. Sweep rate, 100 mV/s.

for  $\text{Co}(\text{phen})_3^{3+}$  was 0.149 V; i.e., the  $\Delta E_{\text{p}}$  values of both couples were not significantly affected by the presence of DNA. However, a large difference was observed in the behavior of the currents of the two redox couples. In the presence of DNA,  $i_{\text{pc}}$  for  $\text{Co}(\text{III})/(\text{II})$  decreased to 36% of that in the absence of DNA, while  $i_{\text{pa}}$  for the  $\text{Mo}(\text{IV})/(\text{V})$  couple was 97% of that in the absence of DNA, when correction was made for the change in background which occurred upon addition of DNA. No significant changes in the steady-state current were observed when the potential was cycled continuously for up to 45 min after the initial scan. Similar results were obtained for  $\text{Fe}(\text{CN})_6^{3-/4-}$  solutions; addition of DNA only slightly affected the current. Thus, a decrease in currents in CV experiments can be attributed to diffusion of the metal complex bound to the large, slowly diffusing DNA molecule. Enhanced viscosity of DNA solutions apparently has only a small effect on diffusion, and there is no significant obstruction of the glassy carbon surface via adsorption of DNA, as opposed to Hg electrodes, where adsorption of DNA at negative potentials is significant.<sup>34</sup>

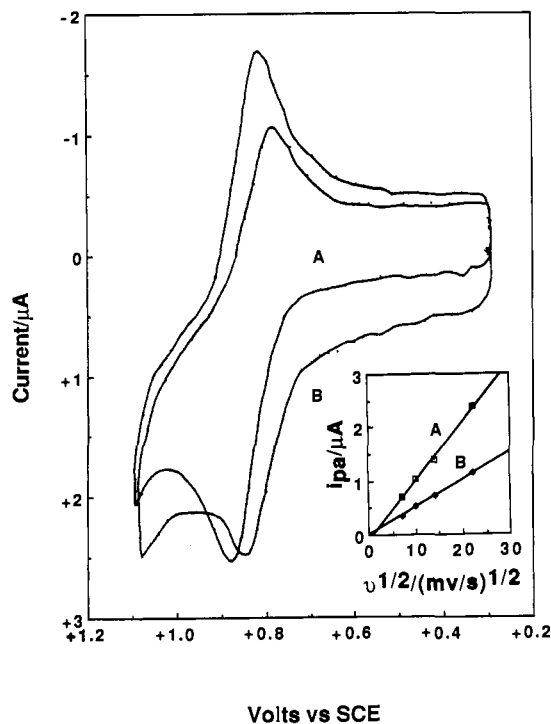


**Figure 6.** Cyclic voltammetry of  $8.1 \times 10^{-5}$  M  $\text{Fe}(\text{bpy})_3^{2+}$  in the (A) absence and (B) presence of 3.84 mM NP. Supporting electrolyte, buffer 2. Sweep rate, 500 mV/s. Inset: Effect of DNA on diffusion of  $\text{Fe}(\text{bpy})_3^{2+}$  at (A)  $R = 0$  and (B)  $R = 66$ .

**$\text{Co}(\text{bpy})_3^{3+/2+}$  and  $\text{Fe}(\text{bpy})_3^{2+/3+}$ .** CV behavior of  $\text{Co}(\text{bpy})_3^{3+}$  ( $1.0 \times 10^{-4}$  M) in the absence and presence of DNA is shown in Figure 5 and that of  $\text{Fe}(\text{bpy})_3^{2+}$  ( $8.1 \times 10^{-5}$  M) in Figure 6. Voltammetric results are presented in Tables IV and V. In the absence of DNA (Figure 5A), reduction of the  $\text{Co}(\text{III})$  species to  $\text{Co}(\text{II})$  occurred at  $E_{\text{pc}} = 0.052$  V and reoxidation at  $E_{\text{pa}} = 0.118$  V ( $\nu = 100$  mV/s);  $E_{1/2} = 0.085$  V. The peak potential separation

(34) (a) Miller, I. R. *J. Mol. Biol.* **1961**, *3*, 229. (b) Miller, I. R.; Bach, D. *Biopolymers* **1966**, *4*, 705. (c) Frei, Y. F.; Miller, I. R. *J. Phys. Chem.* **1965**, *69*, 3018.

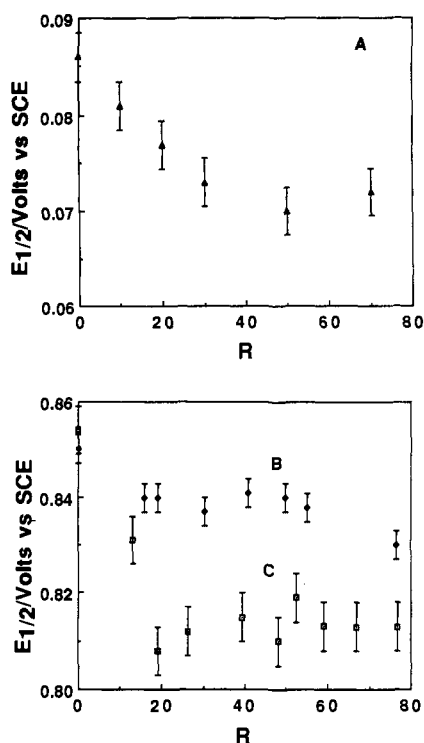


**Figure 7.** Dependence of  $E_{1/2}$  from cyclic voltammetry, on  $R$ , for (A)  $1.0 \times 10^{-4}$  M  $\text{Co}(\text{bpy})_3^{3+}$  (buffer 1), (B)  $7.6 \times 10^{-5}$  M  $\text{Fe}(\text{bpy})_3^{2+}$  (buffer 1), and (C)  $8.1 \times 10^{-5}$  M  $\text{Fe}(\text{bpy})_3^{2+}$  (buffer 2).  $E_{1/2}$  was determined from the average of  $E_{pc}$  and  $E_{pa}$ .

was 66 mV, indicating a fairly reversible electron transfer, as in the case of  $\text{Co}(\text{phen})_3^{3+}$ . In the presence of 5 mM NP (Figure 5B),  $E_{pc}$  shifted to 0.036 V and  $E_{pa}$  to 0.106 V, yielding  $E_{1/2} = 0.071$  V ( $\Delta E_p = 70$  mV). Thus, the apparent  $E_{1/2}$  shifted to more negative potentials by 14 mV in the presence of DNA. CV of  $\text{Fe}(\text{bpy})_3^{2+/3+}$ , at the same supporting electrolyte concentration as for  $\text{Co}(\text{bpy})_3^{3+/2+}$  (buffer 1), gave a small shift in  $E_{1/2}$ . For example, at  $R = 0$   $E_{1/2} = 0.852$  V ( $\Delta E_p = 63$  mV), and at  $R = 41$   $E_{1/2} = 0.840$  V ( $\Delta E_p = 70$  mV). However, more extensive measurements (see below) suggest that the shift in  $E_{1/2}$  is probably less than 10 mV. The peak current for oxidation of the Fe(II) species did not decrease under these conditions, indicating no detectable binding of  $\text{Fe}(\text{bpy})_3^{2+/3+}$  to DNA in buffer 1.

To determine whether any binding of  $\text{Fe}(\text{bpy})_3^{2+}$  could be detected at lower salt concentrations, experiments were carried out in 10 mM NaCl–10 mM Tris, pH 7.1 (buffer 2), (Figure 6). At  $R = 0$ ,  $E_{1/2} = 0.851$  V ( $\Delta E_p = 70$  mV), and at  $R = 47.4$ ,  $E_{1/2} = 0.812$  V ( $\Delta E_p = 70$  mV). Thus, at this lower ionic strength,  $E_{1/2}$  shifted to more negative potentials by 39 mV. The anodic peak current for oxidation of  $\text{Fe}(\text{bpy})_3^{2+}$  decreased to 61% of that in the absence of DNA. These trends suggest much stronger binding of  $\text{Fe}(\text{bpy})_3^{2+}$  to DNA at lower ionic strength. Under these conditions,  $E_{pc}$  and  $E_{pa}$  were independent of  $\nu$ , and  $\Delta E_p$ 's were in the range 62–75 mV.

The behavior of  $E_{1/2}$  of  $\text{Co}(\text{bpy})_3^{3+}$  with varying [NP] is shown in Figure 7A and for  $\text{Fe}(\text{bpy})_3^{2+}$  in Figure 7B,C, for  $0 \leq R \leq 80$ . Little change in  $E_{1/2}$  occurred after ca.  $R = 30$ , as in the case of  $\text{Co}(\text{phen})_3^{3+}$ . The ratio of binding constants for  $\text{Co}(\text{bpy})_3^{3+}$  and  $\text{Co}(\text{bpy})_3^{2+}$   $K_{2+}/K_{3+} = 0.6$ , and so for the bpy complex, the 3+ ion is bound ca. 1.7 times as strongly as the 2+ ion. At low  $\nu$  ( $\leq 100$  mV/s),  $E_p$ 's and  $\Delta E_p$  were essentially independent of  $\nu$ , but at higher values of  $\nu$ , e.g., 500 mV/s to 1.0 V/s,  $\Delta E_p$  values were in the range 83–99 mV and increased with increasing  $\nu$ , indicating the onset of kinetic complications to the electron-transfer steps.<sup>35</sup>  $E_{1/2}$  of  $\text{Fe}(\text{bpy})_3^{2+/3+}$  was essentially unaffected by the presence of DNA in buffer 1 (Figure 7B) but shifted to more negative values by 41 mV in buffer 2, giving  $K_{2+}/K_{3+} = 0.21$ .

Again, little change in  $E_{1/2}$  occurred after  $R = 30$ .

The behavior of  $i_{pc}$  for reduction of  $\text{Co}(\text{bpy})_3^{3+}$  is shown in the inset of Figure 5 and that for oxidation of  $\text{Fe}(\text{bpy})_3^{2+}$  in the inset of Figure 6. For  $\text{Co}(\text{bpy})_3^{3+}$ , in the absence of DNA,  $i_{pc}$  was linear with  $\nu^{1/2}$  for  $5 \leq \nu \leq 500$  mV/s, with zero intercept within the error of the measurement. From this, the free diffusion coefficient for  $\text{Co}(\text{bpy})_3^{3+}$  was calculated as  $D_f = 5.0 (\pm 0.6) \times 10^{-6}$  cm<sup>2</sup>/s. Increasing the concentration of DNA caused suppression of the slope of  $i_{pc}-\nu^{1/2}$ , as observed for  $\text{Co}(\text{phen})_3^{3+}$ . The bound diffusion coefficient,  $D_b$ , was determined to be  $3.2 (\pm 1.0) \times 10^{-7}$  cm<sup>2</sup>/s, from DPV measurements at  $8.0 \times 10^{-6}$  M  $\text{Co}(\text{bpy})_3^{3+}$  and  $R = 1000$ . Thus the apparent diffusion coefficient decreased by a factor of 15.6. Similar results were obtained for  $i_{pa}-\nu^{1/2}$  plots for oxidation of  $\text{Fe}(\text{bpy})_3^{2+}$  (inset of Figure 6), in buffer 2.  $D_f$  was 2.8 ( $\pm 0.6$ )  $\times 10^{-6}$  cm<sup>2</sup>/s from the slope of  $i_{pa}/\nu^{1/2}$  at  $R = 0$ .  $D_b$  was estimated as  $1.8 (\pm 0.6) \times 10^{-7}$  cm<sup>2</sup>/s at  $R = 1037$  and  $1.0 \times 10^{-5}$  M complex.

The ratio  $i_{pa}/i_{pc}$  was less than 1, for  $\text{Co}(\text{bpy})_3^{3+/2+}$ . Rigorous deaeration failed to affect  $i_{pa}/i_{pc}$ . This ratio would be 1 for an uncomplicated redox process. At low  $\nu$  ( $\leq 10$  mV/s,  $R = 0$ ),  $i_{pa}/i_{pc}$  was ca. 0.7 and decreased with increasing  $\nu$ . In the presence of DNA,  $i_{pa}/i_{pc}$  decreased with increasing  $\nu$  and also with increasing [NP]. These results suggest that  $\text{Co}(\text{bpy})_3^{3+}$  is adsorbed on the glassy carbon electrode<sup>36</sup> and that the presence of DNA may enhance this process. A solution of 0.11 mM  $\text{Co}(\text{bpy})_3^{3+}$  was subjected to a 250-ms potential step (chronocoulometry) into the diffusion-controlled region of Figure 5A. The intercept on the charge axis was 0.75  $\mu\text{C}$ . A 0.1 mM  $\text{Co}(\text{phen})_3^{3+}$  solution, however, gave a straight line with approximately the same slope, but which intersected the charge axis at the same point as did a blank experiment, in which only supporting electrolyte was used (0.55  $\mu\text{C}$ ). The excess charge between the intercepts of  $\text{Co}(\text{bpy})_3^{3+}$  and blank experiments (corresponding to a surface excess,  $\Gamma$ , of  $2.95 \times 10^{-11}$  mol/cm<sup>2</sup>), and the lack thereof in the case of  $\text{Co}(\text{phen})_3^{3+}$ , provides evidence for an adsorptive complication to the  $\text{Co}(\text{bpy})_3^{3+}$  voltammetry and the uncomplicated behavior of  $\text{Co}(\text{phen})_3^{3+}$ .<sup>37</sup>  $\text{Co}(\text{bpy})_3^{3+}$  is probably weakly adsorbed at glassy carbon, under these conditions, since  $i_{pa}/i_{pc} < 1$ , but no adsorption postwave is observed.<sup>36</sup> Even if no correction is made for the adsorptive component of the total current for reduction of  $\text{Co}(\text{bpy})_3^{3+}$ , the data indicate that  $\text{Co}(\text{bpy})_3^{3+/2+}$  is moderately strongly bound to DNA, since  $i_{pc}$  decreased to 56% of that in the absence of DNA, for a solution with  $R = 70$  (100 mV/s). Equilibrium binding data for  $\text{Co}(\text{bpy})_3^{3+}$  thus probably represent lower limits of binding parameters, because the small surface excess of oxidized form at the electrode increases the current measured at any  $R$ . The features of the voltammetric behavior of  $\text{Co}(\text{bpy})_3^{3+}$  and  $\text{Fe}(\text{bpy})_3^{2+}$  are summarized in Tables IV and V.

**Titration of Metal Complexes with DNA.** The development of a method to quantify the binding of the electroactive metal complexes to DNA is composed of two parts. First, an equation based on an equilibrium binding model is derived, to compute the relative concentrations of free and DNA-bound complex in bulk solution, as a function of [NP]. Then, voltammetric equations relating the measured value of  $i_{pc}$  or  $i_{pa}$  to mass transfer of the mixture of free and bound metal to the electrode surface must be chosen, depending on whether the exchange of free and bound species is static or mobile (see below) on the time scale of the CV experiment.

We consider the binding of an electroactive metal center, M, to a binding site, S, composed of  $s$  base pairs (bp), residing on the duplex DNA strand (resulting in a bound species, M-S):



The microscopic equilibrium constant for binding is

$$K = C_b / C_f C_s \quad (4)$$

(36) Wopschall, R. H.; Shain, I. *Anal. Chem.* **1967**, *39*, 1514.

(37) Anson, F. C.; Christie, J. H.; Osteryoung, R. A. *J. Electroanal. Chem.* **1967**, *13*, 343.

where  $C_b$ ,  $C_f$ , and  $C_s$  represent the equilibrium concentrations of bound metal, free metal, and free binding sites, respectively. The total concentration of metal,  $C_t$ , is

$$C_t = C_b + C_f \quad (5)$$

and the total concentration of sites along a DNA molecule with an average total number of base pairs  $L$  is

$$xC_{\text{DNA}} = C_b + C_s \quad (6)$$

where

$$x = L/s \quad (7)$$

$$C_{\text{DNA}} = [\text{NP}]/2L \quad (8)$$

Here,  $s$  is the binding site size (in base pairs) of the small molecule interacting with DNA;  $C_{\text{DNA}}$  is the total concentration of DNA strands;  $x$  is the average number of binding sites per molecule of DNA. Solution of eq 4–6 for the concentration of bound complex as a function of  $[\text{NP}]$ , making the appropriate substitutions, eq 7 and 8, to eliminate DNA strand concentration, yields

$$C_b = \frac{b - \left( b^2 - \frac{2K^2 C_t [\text{NP}]}{s} \right)^{1/2}}{2K} \quad (9a)$$

$$b = 1 + KC_t + K[\text{NP}]/2s \quad (9b)$$

$K$  represents the microscopic binding constant for each site; the successive binding constants for 1, 2, ...,  $n$  metal complexes to a DNA molecule will differ from  $K$  by appropriate statistical factors. This is analogous to the well-known situation of proton binding constants in a molecule containing several, noninteracting, basic sites. Equations 9a and 9b are valid for the assumption of non-cooperative, nonspecific binding to DNA with the existence of one type of discrete binding site. While more complex analyses of the binding equilibria are possible,<sup>38</sup> the simple model outlined here adequately describes the voltammetric results.

Under the assumption of reversible, diffusion-controlled electron transfer, two limiting cases may be described for the current in CV, from eq 9, depending on whether the interconversion of free and bound metal, in Scheme I, is treated as static<sup>39</sup> (no interconversion during a scan, eq 10) or mobile<sup>40</sup> (rapid interconversion during a scan, eq 11), on the time scale of the CV experiment:

$$i_{\text{pc}} = B(D_f^{1/2}C_f + D_b^{1/2}C_b) \quad (10)$$

$$i_{\text{pc}} = BC_t(D_f X_f + D_b X_b)^{1/2} \quad (11)$$

where  $i_{\text{pc}}$  is total cathodic current for reduction of the bound and free metal complexes and  $X_f$  and  $X_b$  are the free and bound mole fractions, respectively, of the complex in solution ( $X_f = C_f/C_t$  and  $X_b = C_b/C_t$ ).  $B$  represents the appropriate, concentration-independent terms in the voltammetric expression. For a Nernstian reaction in CV at 25 °C,<sup>32</sup>  $B = 2.69 \times 10^5 n^{3/2} A \nu^{1/2}$ , where  $n$  is the number of electrons transferred per metal complex and  $A$  is the surface area of the glassy carbon disk.

It is of interest to examine the behavior of  $X_b$  as  $R$  is varied over a wide range (at constant  $C_t$ ) and also to examine the voltammetric behavior, in terms of  $i_{\text{pc}}$  vs  $R$ :

$$R = [\text{NP}]/C_t \quad (12)$$

which is predicted by the model under the limiting conditions of eq 10 and 11. Evans has noted the experimental conditions under which each limiting case is justified.<sup>41</sup> Below, we discuss the more

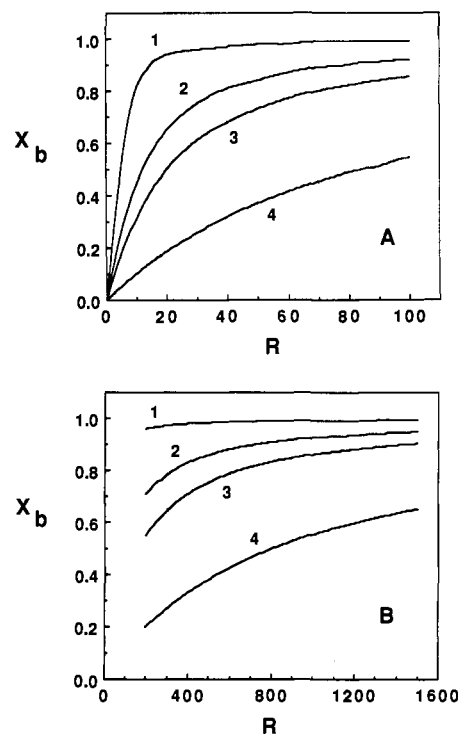


Figure 8. (A) Fraction of metal complex bound to DNA ( $X_b$ ) as a function of  $R$  at  $C_t = 1.0 \times 10^{-4}$  M complex. Curves 1–4 represent  $K = 1 \times 10^5$ ,  $1 \times 10^4$ ,  $5 \times 10^3$ , and  $1 \times 10^3$   $\text{M}^{-1}$ , respectively, for  $s = 4$  bp. (B) Fraction of metal complex bound to DNA as a function of  $R$ , for  $C_t = 1.0 \times 10^{-5}$  M complex. Other parameters are as given in (A).

appropriate limiting case for this work.

The characteristic behavior of the equilibrium binding model is shown in Figure 8. The fraction of electroactive species bound to DNA,  $X_b$ , is shown as a function of  $R$ , for a binding site size ( $s$ ) of 4 bp. Curves 1–4 represent binding constants,  $K$ , of  $1 \times 10^5$ ,  $1 \times 10^4$ ,  $5 \times 10^3$ , and  $1 \times 10^3$   $\text{M}^{-1}$ , respectively, with  $C_t = 1.0 \times 10^{-4}$  M (CV conditions, Figure 8A) or  $1.0 \times 10^{-5}$  M (DPV conditions, Figure 8B). The steepness of the initial rise in  $X_b$  with increasing  $R$  increases as  $K$  becomes larger. At low  $K$ , e.g.,  $1 \times 10^3$   $\text{M}^{-1}$  (Figure 8A, curve 4),  $X_b$  barely reaches 0.5, over the range  $0 \leq R \leq 80$ . For  $K$  between  $5 \times 10^3$   $\text{M}^{-1}$  and  $1.0 \times 10^4$   $\text{M}^{-1}$ ,  $X_b$  reaches 0.8–0.9 over the same range of  $R$ . Thus, under the conditions required for CV measurements, the metal complex–DNA mixture is composed of 80–90% bound complex and 10–20% free complex, for typical values of  $K$ . The largest change in  $X_b$  with increasing  $R$  occurs at  $R \leq 30$ . This is consistent with our observations that little change occurs in  $E_{1/2}$  at  $R > 30$ . Figure 8B shows that for both phen complexes and  $\text{Co}(\text{bpy})_3^{3+}$  (see Table VI) the lower limit on  $X_b$  is ca. 0.8–0.9 (with  $D_b$  measured at  $R \geq 1000$ ).  $\text{Fe}(\text{bpy})_3^{2+}$  binding is much weaker, even at reduced ionic strength, where  $X_b$  is ca. 0.5. Thus, the values of all  $D_b$  measured by DPV contain some contribution from equilibrium free metal. In most cases, reasonable estimates can be obtained. However, the smaller the actual value of  $K$  for a system, the less exact the estimates of  $D_b$  will be, due to limitations imposed by the maximum value of  $R$  that can be attained, as governed by the detection limits of the DPV method and the solubility of DNA. Several other physical contributions to  $D_b$  may exist which can potentially increase its experimentally determined value (see below), which are not related to free electroactive species.

It is also necessary to examine the behavior of the two limiting models, eq 10 and 11. In the limit of no interconversion of bound and free species (in each oxidation state), on the time scale of the CV experiment, the total current is always smaller ( $R > 0$ ) than that in the case of rapid (mobile) interconversion. Thus, assumption of rapid interconversion will yield values of  $K$  that are

(38) McGhee, J. D.; von Hippel, P. H. *J. Mol. Biol.* **1974**, *86*, 469.

(39) Zana, R.; Mackay, R. A. *Langmuir* **1986**, *2*, 109.

(40) (a) Eddowes, M. J.; Grätzel, M. *J. Electroanal. Chem.* **1984**, *163*, 31.

(b) Matsue, T.; Evans, D. H.; Osa, T.; Kobayashi, N. *J. Am. Chem. Soc.* **1985**, *107*, 3411. (c) Kamau, G. N.; Leipert, T.; Shukla, S. S.; Rusling, J. R. *J. Electroanal. Chem.* **1987**, *233*, 173. (d) Rusling, J. F.; Shi, C.-N.; Kumosinski, T. F. *Anal. Chem.* **1988**, *60*, 1260.

(41) Evans, D. H. *J. Electroanal. Chem.* **1989**, *258*, 451.



Table VI. Cyclic Voltammetric Titration of Co(III)/(II) and Fe(II)/(III) Complexes<sup>a,b</sup>

complex	model	experiment <sup>c</sup>				regression <sup>d</sup>				
		$10^6 D_f / \text{cm}^2 \cdot \text{s}^{-1}$	$10^7 D_b / \text{cm}^2 \cdot \text{s}^{-1}$	$10^6 D_f / \text{cm}^2 \cdot \text{s}^{-1}$	$10^7 D_b / \text{cm}^2 \cdot \text{s}^{-1}$	$10^{-3} K_{3+} / \text{M}^{-1}$	$s / \text{bp}$	$K_{2+} / K_{3+}$	$10^{-3} K_{2+} / \text{M}^{-1}$	
Co(phen) <sub>3</sub> <sup>3+</sup>	static	3.7 (0.3)	2.6 (0.3)	4.2	2.6	16 (2)	6	1.94	30	
	mobile	3.7 (0.3)	2.6 (0.3)	4.2	2.6	26 (4)	5	1.94	51	
Co(bpy) <sub>3</sub> <sup>3+</sup>	static	5.0 (0.3)	3.2 (1.0)	4.5	12	9.4 (1.5)	3	0.58	5.4	
	mobile	5.0 (0.3)	3.2 (1.0)	4.5	12	14 (3)	3	0.58	8.4	
Fe(phen) <sub>3</sub> <sup>2+</sup>	static	4.9 (0.5)	0.9 (0.04)	4.9	0.9	7.1	5	1	7.1 (0.2)	
	mobile	4.9 (0.5)	0.9 (0.04)	4.9	0.9	14.7	4	1	14.7 (0.4)	
Fe(bpy) <sub>3</sub> <sup>2+</sup>	static	2.8 (0.3)	1.8 (0.3)	2.8	1.8	5.0	4	0.21	1.1 (0.6)	
	mobile	2.8 (0.3)	1.8 (0.3)	2.8	1.8	6.6	3	0.21	1.4 (0.1)	

<sup>a</sup> [Co(phen)<sub>3</sub><sup>3+</sup>] =  $1.0 \times 10^{-4}$  M; [Co(bpy)<sub>3</sub><sup>3+</sup>] =  $1.0 \times 10^{-4}$  M. Supporting electrolyte, 50 mM NaCl + 5 mM Tris, pH 7.1. Sweep rate, 100 mV/s. <sup>b</sup> Fe(phen)<sub>3</sub><sup>2+</sup>:  $3.43 \times 10^{-5}$  mol of NP titrated with 0.69 mM complex. Supporting electrolyte, 50 mM NaCl + 5 mM Tris, pH 7.1. Fe(bpy)<sub>3</sub><sup>2+</sup>:  $3.83 \times 10^{-5}$  mol of NP titrated with 0.75 mM complex. Supporting electrolyte, 10 mM NaCl + 10 mM Tris, pH 7.1. Sweep rate, 500 mV/s. <sup>c</sup> Numbers in parentheses are standard deviations of experimental measurements. <sup>d</sup> Numbers in parentheses represent 95% confidence interval of parameter estimate from nonlinear regression.

larger than those predicted by the static limit, given the same diffusional parameters and binding site size. For our systems, the two limiting cases give experimental  $K$  values which differ by no more than a factor of 2.0. It is difficult to determine exactly the more appropriate model for the measured current, since the reduction processes of free and bound material are not well resolved. Thus, we present results for calculations of both limiting cases.

Finally, some qualitative aspects of the influence of  $K$ ,  $s$ , and  $D_b$  on the modeling of the binding equilibrium are presented, to determine how to choose the best-fit parameters in the most judicious fashion. The end point of the titration curve becomes more pronounced as  $K$  is increased. At binding constants of  $<10^3 \text{ M}^{-1}$ , the curve is barely distinguishable from a straight line, and no useful information can be obtained in this binding regime. The degree of decrease in current, compared to a solution without added DNA, is also dependent on  $D_b$ . Changes in the magnitude of  $D_b$  cause no major changes in the curvature of the titration curve in the region of the end point, but they change the point at which the current no longer decreases significantly (e.g., in experiments where decrease in current is plotted as a function of increasing  $R$ , at constant  $C_i$ ). The ratio  $D_f/D_b$  and the accuracy with which  $D_b$  can be measured will ultimately be limited by the limiting factors in the definition of the binding curve and thus in the ability to fit curves for values of  $K$  and  $s$ . It is always desirable to have systems in which  $D_f/D_b$  values are as large as possible. In our studies, experimentally determined ratios are between 14 and 55; these are large enough to yield useful titration curves. The determination of  $s$  presents the most difficulty, since it (1) changes the degree of curvature at the end point, (2) changes the point at which the current stops decreasing significantly, and (3) changes the position of the end point along the  $R$  axis. Effect 3 is expected, since  $s$  determines the end point of the titration experiment. However, effects 1 and 2 suggest that  $s$  is correlated with both  $K$  and  $D_b$  and thus cannot reliably be fitted simultaneously with the other parameters of interest. Our approach was to set  $D_f$  and  $D_b$  (adjusted only within the limits of their experimental determination) and regress current-[NP] (or current- $C_i$ ) data onto eq 8 and either 10 or 11, for integer values of  $s$ . The best fit of the parameters to the experimental data was taken as those corresponding to the value of  $s$ , which yielded the minimum sum of squares deviation, between the experimental and calculated currents, with  $s$  varied over a sufficiently wide range (e.g.,  $1 \text{ bp} \leq s \leq 20 \text{ bp}$ ).

Results for the titration of 0.1 mM Co(phen)<sub>3</sub><sup>3+</sup> and 0.1 mM Co(bpy)<sub>3</sub><sup>3+</sup> with DNA are shown in Figure 9. The supporting electrolyte in both cases was buffer 1, and the best-fit curves shown are for the mobile equilibrium limit. Complete results of nonlinear regression analysis of the titration data are summarized in Table VI. The values of  $K_{2+}$  were obtained from the  $K_{2+}/K_{3+}$  ratio determined from the shift of  $E_{1/2}$ . Analogous titration experiments are shown in Figure 10 for experiments with Fe(phen)<sub>3</sub><sup>2+</sup> (Figure 10A) and Fe(bpy)<sub>3</sub><sup>2+</sup> (Figure 10B). The curves shown are for mobile exchange; complete results are given in Table VI. In these cases the experiment was performed differently from those in Figure 9; a solution initially containing only DNA was titrated

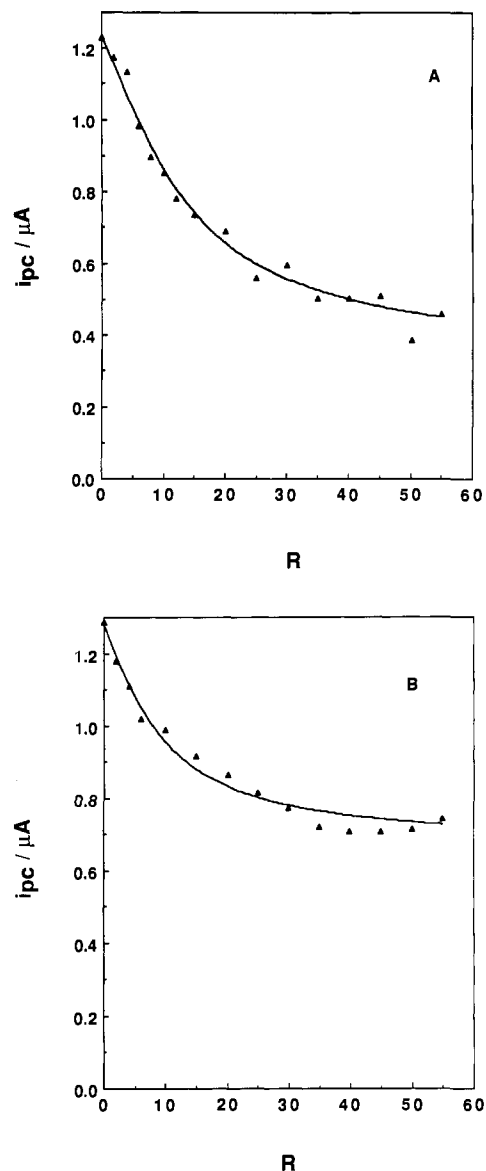
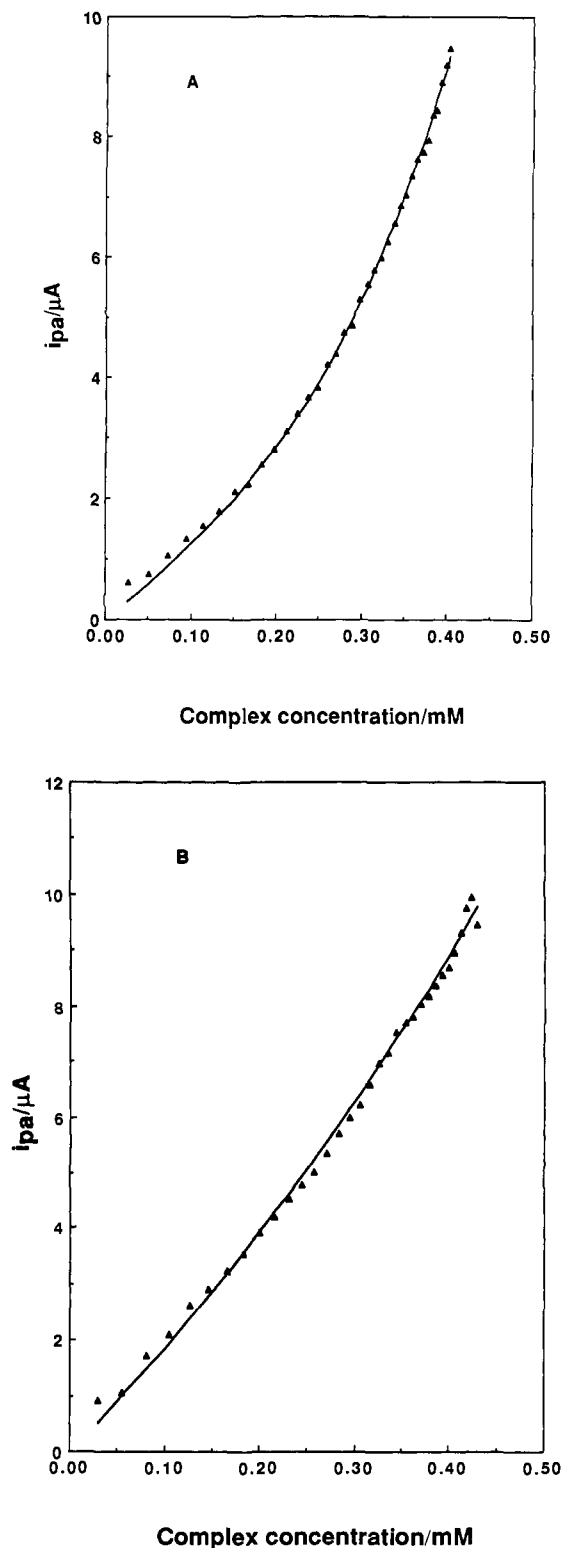


Figure 9. Titration of (A)  $1.0 \times 10^{-4}$  M Co(phen)<sub>3</sub><sup>3+</sup> and (B)  $1.0 \times 10^{-4}$  M Co(bpy)<sub>3</sub><sup>3+</sup> with DNA. Points represent experimental data, and the solid curve represents the results for best-fit parameters with consideration of the mobile equilibrium limiting case, as given in the text. Sweep rate, 100 mV/s. Supporting electrolyte, buffer 1.

with the metal complex. Exactly the same information about binding is obtained from this experiment. Binding of the Fe complexes is weaker in each ligand case than that of the corresponding Co complexes. These differences probably reflect different contributions to binding by both electrostatic and inter-



**Figure 10.** Titration of (A)  $3.43 \times 10^{-5}$  mol of NP with 0.68 mM  $\text{Fe}(\text{phen})_3^{2+}$  and (B)  $3.83 \times 10^{-5}$  mol of NP with 0.75 mM  $\text{Fe}(\text{bpy})_3^{2+}$ . Points represent experimental data, and the solid curve represents the best fit for the binding parameters given in the text, with consideration of the mobile equilibrium limiting case. Supporting electrolyte, buffer 2. Sweep rate, 500 mV/s. Initial solution volume, 5 mL.

calative components of the interactions of these complexes with DNA, as discussed in detail in the following section.

#### Discussion

**Differentiation of Intercalative and Coulombic Interactions.** The shifts in the formal potential,  $E^{\circ'}$ , of the  $\text{M}(\text{phen})_3^{3+/2+}$  and  $\text{M}(\text{bpy})_3^{3+/2+}$  redox couples can be understood in terms of the

predominant mode of interaction of each complex with the DNA strand.

As shown by Barton,<sup>2a,d</sup> tris-chelated transition-metal complexes with phen ligands bind to DNA by intercalation, with partial insertion of one of the ligands between adjacent base pairs on the DNA duplex strand. The remaining ligands are disposed along the major groove of the DNA molecule, and therefore, the complex can interact electrostatically with the sugar-phosphate backbone and hydrophobically with the environment in the region of the paired nucleotide bases.

The configuration of the metal complex, when in contact with the DNA helix, has been deduced for  $\text{Ru}(\text{phen})_3^{2+}$  and  $\text{Ru}(\text{DIP})_3^{2+}$  (DIP = 4,7-diphenyl-1,10-phenanthroline).<sup>5a-c</sup> Similar binding has been suggested for  $\text{Fe}(\text{phen})_3^{2+}$ .<sup>7</sup> The structurally analogous complexes of Co(III) probably bind by partial ligand intercalation and dispose themselves along the DNA molecule in a similar fashion, since their enantiospecificity toward B-form vs Z-form DNA and ability to unwind supercoiled, closed circular DNA are directly analogous to the ruthenium(II) cases.<sup>13</sup> The noncovalent interaction of the intercalating ligand with the DNA base pairs<sup>2b,c</sup> and the concomitant disposition of the remaining ligands along the groove<sup>5h</sup> brings the  $\text{Co}(\text{phen})_3^{3+}$  complex into close contact with an environment that is hydrophobic compared to the region of the charged sugar-phosphate backbone. The hydrophilic coat/hydrophobic core structure of the DNA molecule has been discussed previously.<sup>42</sup> The interplay between electrostatic and hydrophobic (intercalative) interactions therefore can be important in the overall binding of a charged species which possesses a planar, aromatic moiety.<sup>2c,43</sup>

The limiting shift in  $E^{\circ'}$  of +17 mV for the  $\text{Co}(\text{phen})_3^{3+/2+}$  couple ( $0 \leq R \leq 90$ ) shows, via eq 2, that the 2+ ion is bound to DNA 1.94 times more strongly than the 3+ ion. This suggests that the intercalated complex interacts predominantly with the hydrophobic interior of the DNA strand, so that reduction of the 3+ ion is facilitated compared to that of a solution that does not contain DNA. Electrochemical effects influenced by hydrophobic interactions of charged, electroactive molecules with hydrophobic or amphiphilic host matrices have been described previously, e.g., for the interactions of viologens and metal chelates with micelles<sup>33,40c,44</sup> and perfluorosulfonated (Nafion) polymers.<sup>45</sup> For example, the 1+ form of 1-decyl-1'-methyl-4,4'-bipyridinium binds more strongly to Triton X-100 micelles than the 2+ form.<sup>44a</sup>  $\text{Os}(\text{bpy})_3^{2+}$  binds to SDS (sodium dodecyl sulfate) micelles more strongly than  $\text{Os}(\text{bpy})_3^{3+}$ ,<sup>44b</sup> and  $\text{MV}^+$  (MV = methylviologen, 1,1'-methyl-4,4'-bipyridinium) binds more strongly than  $\text{MV}^{2+}$  to SDS.<sup>33</sup>  $\text{Ru}(\text{bpy})_3^{2+}$  associates more strongly than the 3+ cation with Nafion.<sup>45</sup> Hydrophobic interactions have also been implicated in the association of  $\text{CoL}_3^{2+}$  (where L = bpy or 4,4'-dimethyl-bpy) with CTAB (cetyltrimethylammonium bromide) micelles.<sup>46</sup> These examples show that hydrophobic interactions, in which reduction of the total charge on the electroactive species yields stronger binding in the hydrophobic domain of the host matrix, can be important in describing the binding of a charged molecule to an amphiphilic matrix, and in many cases these interactions can overcome simple coulombic interactions (e.g., between a positively charged metal complex and a negatively charged SDS micelle or in this case the negatively charged sugar-phosphate backbone of DNA). The nature of the solvent can have substantial effects on electron-transfer thermodynamics.<sup>47</sup> The DNA strand may be considered as a local "solvent" environment, as far as bound metal

(42) (a) Fromhertz, P.; Rieger, B. *J. Am. Chem. Soc.* **1986**, *108*, 5361. (b) Flöser, G.; Haarer, D. *Chem. Phys. Lett.* **1988**, *147*, 288. (c) Patel, D. J.; Kozłowski, S. A.; Rice, J. A. *Proc. Natl. Acad. Sci. U.S.A.* **1981**, *78*, 3333.

(43) (a) Zimmerman, H. W. *Angew. Chem., Int. Ed. Engl.* **1986**, *25*, 115. (b) Feigon, J.; Denny, W. A.; Leupin, W.; Kearns, D. R. *J. Med. Chem.* **1984**, *27*, 450. (c) Fromhertz, P. *Chem. Phys. Lett.* **1984**, *109*, 407.

(44) (a) Hoshino, K.; Sasaki, H.; Suga, K.; Saji, T. *Bull. Chem. Soc. Jpn.* **1987**, *60*, 1521. (b) Ouyang, J.; Bard, A. J. *Bull. Chem. Soc. Jpn.* **1988**, *61*, 17.

(45) Martin, C. R.; Rubinstein, I.; Bard, A. J. *J. Am. Chem. Soc.* **1982**, *104*, 4817.

(46) Kamau, G. N.; Leipert, T.; Shukla, S. S.; Rusling, J. F. *J. Electroanal. Chem.* **1987**, *233*, 173.

(47) Sahami, S.; Weaver, M. J. *J. Electroanal. Chem.* **1981**, *122*, 155.

complex is concerned, which differs from the bulk medium in dielectric constant and charge distribution. In fact, an increase in the hydrophobic character of the bulk solvent via addition of alcohols can effectively decrease the binding of the strongly intercalating ethidium cation to DNA.<sup>48</sup> However, since many systems that demonstrate intercalation also show ionic strength dependent binding,<sup>5c,g,7,49</sup> there is generally an interplay between electrostatic and hydrophobic interactions, even in systems in which intercalation is evident. The degree to which hydrophobic interactions predominate over electrostatic ones is likely to be dictated by structural, geometric, and charge considerations for the binding molecule. Since the  $\text{Fe}(\text{phen})_3^{2+/3+}$  couple shows weaker binding than the corresponding  $\text{Co}(\text{III})/(\text{II})$  couple and no preference of either the oxidized or reduced form for DNA, under the same experimental conditions, for  $\text{Fe}(\text{phen})_3^{2+/3+}$  the intercalative component of binding is probably less important than in  $\text{Co}(\text{phen})_3^{3+/2+}$ . One possible explanation of this effect is that the intercalating phen ligand penetrates between adjacent base pairs on DNA to a smaller extent in the  $\text{Fe}(\text{II})$  case than in the  $\text{Co}(\text{III})$  case.

Tris-chelated metal complexes possessing bpy ligands bind to DNA predominantly via electrostatic intercalations with the negatively charged deoxyribose-phosphate backbone.<sup>5c,e,i,7</sup> The smaller size of the bpy ligand vs phen and slight nonplanarity of the ligand preclude effective intercalation between adjacent base pairs on DNA.<sup>5c</sup> For example,  $\text{Ru}(\text{bpy})_3^{2+}$  does not unwind poly[d(G-C)] or poly[d(A-T)], and its excited-state luminescence is rapidly quenched by ferrocyanide in the presence of DNA, as opposed to that of  $\text{Ru}(\text{phen})_3^{2+}$ , which is protected from quenching while intercalated into DNA.<sup>5c</sup> These observations, in addition to the ionic strength dependence of the binding of bpy-ligated complexes to DNA,<sup>5c,i</sup> support the conclusion that the bpy complexes reside primarily at the outer, hydrophilic coat of the DNA helix, with no significant intercalative component to the binding process. The shift of  $E^\circ$  for  $\text{Co}(\text{bpy})_3^{3+/2+}$  to more negative potentials by  $-14$  mV ( $K_{2+}/K_{3+} = 0.6$ , buffer 1) and of  $\text{Fe}(\text{bpy})_3^{2+/3+}$  by  $-41$  mV ( $K_{2+}/K_{3+} = 0.21$ , buffer 2) indicates that the  $3+$  ion is bound more strongly than the  $2+$  ion in each case. This is consistent with electrostatic binding of  $\text{M}(\text{bpy})_3^{3+/2+}$  to DNA via the anionic phosphate residues with release of  $\text{Na}^+$  counterions from the DNA strand.<sup>50</sup>

**Comparison to Previous Studies.** Binding of a number of other metal chelates with DNA has been studied previously. For example, the  $\text{Ru}(\text{phen})_3^{2+}$  complex, whose binding constant  $K_{2+}$  has been measured by equilibrium dialysis ( $6.2 \times 10^3 \text{ M}^{-1}$  in 50 mM  $\text{NaCl}$ <sup>5a</sup> and  $2.13 \times 10^3 \text{ M}^{-1}$  in 100 mM  $\text{NaCl}$ <sup>5b</sup>), binds less strongly than the corresponding Fe and Co species. However, the  $\text{Pt}(\text{I})$  complex,  $\text{Pt}(\text{en})(\text{phen})^+$  binds more strongly;  $K_+ = 1.8 \times 10^5 \text{ M}^{-1}$  in 100 mM  $\text{NaCl}$ .<sup>51</sup> The binding of  $\text{Ru}(\text{bpy})_3^{2+}$ , which like the bpy complexes of Co and Fe involves mainly electrostatic interactions, has been studied at different ionic strengths. No detectable binding of  $\text{Ru}(\text{bpy})_3^{2+}$  to DNA was observed in 50 mM  $\text{NaCl}$ ,<sup>5c</sup> while at 10 mM phosphate buffer some weak binding has been observed,<sup>5c</sup> but not precisely quantitated.  $K_{2+}$  for  $\text{Ru}(\text{bpy})_3^{2+}$  is  $2 \times 10^5 \text{ M}^{-1}$  at an ionic strength less than 5 mM,<sup>51</sup> with  $s = 1.5$  bp. Other workers have reported  $K_{2+}$  of  $\text{Ru}(\text{bpy})_3^{2+}$  to be  $3.0 \times 10^6 \text{ M}^{-1}$  ( $s = 10$  bp) at 1.0 mM  $\text{NaCl}$  and  $1.4 \times 10^6 \text{ M}^{-1}$  ( $s = 25$  bp) at 10.0 mM  $\text{NaCl}$ .<sup>7</sup> In general, the values of  $s$  for the bpy complexes are smaller than those of the corresponding phen complexes, perhaps reflecting the slightly smaller size of the bpy complexes.

The relative magnitudes of the binding constants for the structurally similar complexes here agree with the concept that interactions involving intercalation are usually stronger than the corresponding purely electrostatic ones under equivalent exper-

imental conditions. The binding constants obtained here are the averages of the behavior expected for pure  $\Delta$  and  $\Lambda$  enantiomers of the complexes, especially in the case of  $\text{M}(\text{phen})_3^{n+}$ . Binding of racemic  $\text{Ru}(\text{phen})_3^{2+}$  to DNA was intermediate between that of the  $\Delta$  and  $\Lambda$  enantiomers.<sup>2a,d</sup> The binding constants are also smaller than those obtained for the classical intercalators, e.g., ethidium and proflavin, where complete insertion of the planar molecules between base pairs is possible.<sup>2b</sup> For example,  $K_+$  for ethidium is  $7 \times 10^7 \text{ M}^{-1}$  in 40 mM Tris-HCl buffer, pH 7.9,<sup>49b</sup> and  $1.4 \times 10^6 \text{ M}^{-1}$  in 40 mM  $\text{NaCl}$ -25 mM Tris-HCl,<sup>49c</sup> and proflavin binds with  $K = 4.1 \times 10^5 \text{ M}^{-1}$  (*Escherichia coli* DNA, 50% GC content) in 0.1 M Tris-HCl.<sup>52</sup>

**Mass Transfer and Equilibrium Considerations.** To our knowledge, no kinetic data are available for determining the appropriate limiting case (static or mobile) for exchange of free and bound metal complex, in each oxidation state, and the more appropriate eq 10 or 11, for use in the analysis. We suggest, however, that the mobile limit (rapid interconversion of free and bound complex on the time scale of the voltammetric measurement) may be the more accurate representation of these systems, since no appreciable kinetic limitations to the redox reactions were observed in  $i_{pc}^{-\nu^{1/2}}$  trends or in the dependence of  $\Delta E_p$  on  $\nu$ . Kinetic contributions from rate-limiting exchange of free and bound complex would be expected to give significantly broader  $\Delta E_p$  values than those observed here,<sup>44,53</sup> on the basis of the proposed reaction scheme. The diffusion coefficients of bound metal complex, measured by DPV, are somewhat larger than those previously reported for analogous samples of calf thymus DNA, where diffusion coefficients have been previously reported as  $9.2 \times 10^{-8} \text{ cm}^2/\text{s}$ <sup>34b</sup> and  $1.3 \times 10^{-8} \text{ cm}^2/\text{s}$ .<sup>54</sup> The increase in magnitude of  $D_b$  can be explained by the existence of a small equilibrium concentration of free metal complex. This will exaggerate the value of  $D_b$ . Since the binding constants of systems such as those studied here are rather small (typically  $\leq 3.0 \times 10^4 \text{ M}^{-1}$ ), the presence of equilibrium free metal will always compromise the determination of  $D_b$ , although relatively reliable estimates may be obtained. Since the DNA samples are probably polydisperse, diffusion of metal complex bound to small, more rapidly diffusing fragments may also contribute to enhancement of  $D_b$ . Facilitated diffusion along the DNA strand,<sup>55</sup> which has not been examined in this work, cannot be ruled out as a further contribution to  $D_b$ .

## Conclusions

Electrochemical methods have been used to probe the mode of interaction of  $\text{M}(\text{phen})_3^{3+/2+}$  and  $\text{M}(\text{bpy})_3^{3+/2+}$  with DNA, where  $\text{M} = \text{Co}$  or  $\text{Fe}$ . Shifts in  $E^\circ$  can be used to differentiate intercalative interactions, which involve hydrophobic interactions with the interior of the DNA molecule, from electrostatic ones, which involve the outer anionic coat of DNA. Binding parameters for multiple oxidation states can be obtained from the dependence of peak current on the ratio of nucleotide phosphate to metal from titration experiments.  $\text{Co}(\text{phen})_3^{3+}$  binds intercalatively to DNA, with the reduced ( $2+$ ) form associating more strongly than the oxidized form. For  $\text{Fe}(\text{phen})_3^{2+}$ , no charge preference was found.  $\text{Co}(\text{bpy})_3^{3+}$  and  $\text{Fe}(\text{bpy})_3^{2+}$  bind via electrostatic interaction, where the oxidized ( $3+$ ) form is bound more strongly.  $\text{Fe}(\text{bpy})_3^{2+}$  displays a marked ionic strength dependence of its binding to DNA. No binding is observed in 50 mM  $\text{NaCl}$ , whereas  $\text{Co}(\text{bpy})_3^{3+}$  binds moderately, under these conditions.

**Acknowledgment.** The support of the National Science Foundation (CHE8402135) and an NSF Minority Graduate Fellowship to M.R. are gratefully acknowledged.

**Registry No.**  $\text{Co}(\text{phen})_3^{3+}$ , 18581-79-8;  $\text{Fe}(\text{phen})_3^{2+}$ , 14708-99-7;  $\text{Co}(\text{bpy})_3^{3+}$ , 19052-39-2;  $\text{Fe}(\text{bpy})_3^{2+}$ , 15025-74-8.

(48) Baldini, G.; Varani, G. *Biopolymers* **1985**, *25*, 2187.

(49) (a) Lerman, L. S. *J. Mol. Biol.* **1961**, *3*, 18. (b) Waring, M. J. *J. Mol. Biol.* **1965**, *13*, 269. (c) LePecq, J.-B.; Paoletti, C. *J. Mol. Biol.* **1967**, *27*, 87. (d) Pauluhn, J.; Zimmermann, H. W. *Ber. Bunsen-Ges. Phys. Chem.* **1978**, *82*, 1265.

(50) Manning, G. S. *Q. Rev. Biophys.* **1978**, *11*, 179.

(51) Howe-Grant, M.; Lippard, S. J. *Biochemistry* **1979**, *18*, 5762.

(52) Baba, Y.; Beatty, C. L.; Kagemoto, A. In *Biological Activities of Polymers*; Carreher, C. E., Jr.; Gebelein, C. G., Eds.; ACS Symposium Series 186, American Chemical Society: Washington, DC, 1982; Chapter 14, pp 177-189.

(53) Matsue, T.; Evans, D. H. *J. Electroanal. Chem.* **1984**, *168*, 287.

(54) Tanford, C. *Physical Chemistry of Macromolecules*; Wiley: New York, **1961**; Chapter 5, p 361.

(55) Berg, O. G.; von Hippel, P. H. *Annu. Rev. Biophys. Biophys. Chem.* **1985**, *14*, 131.